



1 **Synthetic ozone deposition and stomatal uptake at flux tower sites**

2 Jason A. Ducker¹, Christopher D. Holmes¹, Trevor F. Keenan^{2,3}, Silvano Fares⁴, Allen H.
3 Goldstein³, Ivan Mammarella⁵, J. William Munger⁶, Jordan Schnell⁷

4

5 ¹ Department of Earth, Ocean, and Atmospheric Science, Florida State University, Tallahassee,
6 Florida

7 ² Lawrence Berkeley National Laboratory, University of California, Berkeley, California

8 ³ Department of Environmental Science, Policy, and Management, University of California,
9 Berkeley, California

10 ⁴ Council of Agricultural Research and Economics (CREA), Research Centre for Forestry and
11 Wood, Arezzo, Italy.

12 ⁵ Institute for Atmosphere and Earth System Research/Physics, PO Box 68, Faculty of Science,
13 University of Helsinki, Finland

14 ⁶ Department of Earth and Planetary Sciences, Northwestern University, Evanston, Illinois

15

16 ⁷ NOAA Geophysical Fluid Dynamics Laboratory, Princeton, New Jersey

17

18 **Abstract**

19

20 We develop and evaluate a method to estimate O₃ deposition and stomatal O₃ uptake across
21 networks of eddy covariance flux tower sites where O₃ concentrations and O₃ fluxes have not
22 been measured. The method combines standard micrometeorological flux measurements, which
23 constrain O₃ deposition velocity and stomatal conductance, with a gridded dataset of observed
24 surface O₃ concentrations. Measurement errors are propagated through all calculations to
25 quantify O₃ flux uncertainties. We evaluate the method at three sites with O₃ flux measurements:
26 Harvard Forest, Blodgett Forest, and Hyttiälä Forest. The method reproduces 83% or more of
27 the variability in daily stomatal uptake at these sites with modest mean bias (21% or less). At
28 least 95% of daily average values agree with measurements within a factor of two and, according
29 to the error analysis, the residual differences from measured O₃ fluxes are consistent with the
30 uncertainty in the underlying measurements.

31

32 The product, called synthetic O₃ flux or SynFlux, includes 43 FLUXNET sites in the United
33 States and 60 sites in Europe, totaling 926 site-years of data. This dataset, which is now public,
34 dramatically expands the number and types of sites where O₃ fluxes can be used for ecosystem
35 impact studies and evaluation of air quality and climate models. Across these sites, the mean
36 stomatal conductance and O₃ deposition velocity is 0.03-1.0 cm s⁻¹. The stomatal O₃ flux during
37 the growing season (April-September) is 0.5-11.0 nmol m⁻² s⁻¹ with a mean of 4.5 nmol m⁻² s⁻¹
38 and the largest fluxes generally occur where stomatal conductance is high, rather than where O₃
39 concentrations are high. The conductance differences across sites can be explained by
40 atmospheric humidity, soil moisture, vegetation type, irrigation, and land management. These



41 stomatal fluxes suggest that ambient O₃ degrades biomass production and CO₂ sequestration by
42 20-24% at crop sites, 6-29% at deciduous broadleaf forests, and 4-20% at evergreen needleleaf
43 forests in the United States and Europe.

44

45 1 Introduction

46

47 Surface ozone (O₃) is toxic to both people and plants. Present-day and recent historical O₃ levels
48 reduce carbon sequestration in the biosphere (Reich and Lassoie, 1984; Guidi et al., 2001; Sitch
49 et al., 2007; Ainsworth et al., 2012), perturb the terrestrial water cycle (Lombardozzi et al., 2012,
50 2015), and cause around \$25 billion in annual crop losses (Reich and Amundson, 1985; Van
51 Dingenen et al., 2009; Avnery et al., 2011; Tai et al., 2014). The basic plant responses to O₃
52 injury are well established from controlled exposure experiments (e.g. Wittig et al., 2009;
53 Ainsworth et al., 2005, 2012; Hoshika et al., 2015) but few datasets are available to quantify O₃
54 fluxes and responses for whole ecosystems or plant functional types that are represented within
55 regional and global biosphere and climate models. The eddy covariance method has been widely
56 used to measure land-atmosphere fluxes of carbon, water, and energy and evaluate their
57 representation in models (Baldocchi et al., 2001; Bonan et al., 2011), but few towers measure O₃
58 fluxes (Munger et al., 1996; Fowler et al., 2001; Keronen et al., 2003; Gerosa et al., 2004;
59 Lamaud et al., 2009; Fares et al., 2010; Stella et al., 2014; Zona et al., 2014). A recent review
60 identified just 78 field measurements of O₃ fluxes over vegetation during the last 4 decades,
61 many lasting just a few weeks (Silva and Heald, 2017). This paper demonstrates a reliable
62 method to estimate O₃ fluxes at 103 eddy covariance flux towers spanning over two decades to
63 enable O₃ impact studies on ecosystem scales.

64

65 The land surface is a terminal sink for atmospheric O₃ due to the reactivity of O₃ with
66 unsaturated organic molecules and the modest solubility of O₃ in water. Surface deposition
67 removes about 20% of tropospheric O₃, making it an important control on air pollution (Wu et
68 al., 2007; Young et al., 2013, Kavassalis and Murphy, 2017). This O₃ deposition flux includes
69 stomatal uptake into leaves, where O₃ can cause internal oxidative damage, and less harmful
70 non-stomatal deposition to plant cuticles, stems, bark, soil, and standing water (Fuhrer, 2000;
71 Zhang et al., 2002; Ainsworth et al., 2012). O₃ can also react with biogenic volatile organic
72 compounds in the plant canopy air and this process is commonly included in non-stomatal
73 deposition (Kurpius and Goldstein, 2003). The deposition flux (mol m⁻² s⁻¹) can be described as:

$$F_{O_3} = v_d n (\chi - \chi_0) = v_d n \chi \quad (1)$$

74 where χ and χ_0 are the O₃ mole fractions (mol mol⁻¹) in the atmosphere and at the surface,
75 respectively, n is the molar density of air (mol m⁻³), and v_d is a deposition velocity (m s⁻¹) that
76 expresses the net vertical O₃ transport between the height where χ is measured and the surface.
77 F_{O_3} is defined positive for flux towards the ground. Eq. 1 reasonably assumes that $\chi_0 = 0$ because
78 terrestrial surfaces have abundant organic compounds that react with and destroy O₃. The
79 deposition velocity can be decomposed into resistances (s m⁻¹) for aerodynamic transport (r_a),
80



81 diffusion in the quasi-laminar layer (r_b), stomatal uptake (r_s), and non-stomatal deposition (r_{ns})
82 (Wesely, 1989):

$$v_d^{-1} = r_a + r_b + (r_s^{-1} + r_{ns}^{-1})^{-1}. \quad (2)$$

83 For stomatal and non-stomatal processes, the rates are often expressed as conductances (m s^{-1}),
84 which are the inverse of the resistances: $g_s = r_s^{-1}$ and $g_{ns} = r_{ns}^{-1}$. The sum of stomatal and non-
85 stomatal conductances is the vegetation canopy conductance, $g_c = g_s + g_{ns}$. The stomatal O₃
86 flux is the portion of F_{O_3} that enters the stomata, and can be described as:

$$F_{s,\text{O}_3} = F_{\text{O}_3} g_s (g_s + g_{ns})^{-1} = v_d n \chi g_s (g_s + g_{ns})^{-1}. \quad (3)$$

87
88 To construct the synthetic O₃ flux, or SynFlux, we use measurements of O₃ concentration and
89 standard eddy covariance flux measurements to derive nearly all of the terms in Eqs. 1-3 from
90 surface observations, using minimal additional information from remote sensing and models.
91 This enables the estimation of F_{O_3} and F_{s,O_3} , as described in Section 2. In Section 3 we then
92 evaluate the method against observations at three sites that measure F_{O_3} , examine the importance
93 of stomatal and non-stomatal deposition, and compare flux-based metrics of O₃ damage with
94 concentration-based metrics. Finally, we discuss the strengths, limitations, and implications of
95 our approach in Section 4.
96
97

98 2 Data sources and methods

99

100 2.1 SynFlux: synthetic O₃ flux

101

102 The FLUXNET2015 dataset (Pastorello et al., 2017) aggregates measurements of land-
103 atmosphere fluxes of CO₂, H₂O, momentum, and heat at sites around the world
104 (<http://fluxnet.fluxdata.org/data/fluxnet2015-dataset>, accessed 24 February 2017). Measurements
105 are made with the eddy covariance method on towers above vegetation canopies (Balocchi et
106 al., 2001; Anderson et al., 1984; Goldstein et al., 2000) with consistent gap-filling (Reichstein et
107 al., 2005; Vuichard and Papale, 2015) and quality control across sites (Pastorello et al., 2014).
108 Flux and meteorological quantities are reported in half hour intervals. We analyze data from all
109 sites in the United States and Europe in the FLUXNET2015 Tier 1 dataset. This analysis is
110 restricted to the US and Europe because these regions have dense O₃ monitoring networks,
111 described below. There are 103 sites meeting these criteria, all listed in Table S1 with references
112 to full site descriptions. Three of these sites—Blodgett Forest, Harvard Forest, and Hyytiälä
113 Forest—measure O₃ flux with the eddy covariance method, which we will use in Sect. 3 to
114 evaluate our methods.
115

116

117 SynFlux aims to tightly constrain O₃ deposition resistances using measured water, heat and
118 momentum fluxes, in contrast to other methods that rely more heavily on atmospheric models or
119 standard meteorology observations (Finkelstein et al., 2000; Mills et al. 2011; Schwede et al.,
120 2011; Yue et al., 2014). From the eddy covariance measurements, we derive the resistance



121 components of Eq. 2 using methods similar to past studies (Kurpius and Goldstein, 2003; Gerosa
122 et al., 2005; Fares et al., 2010). The aerodynamic and quasi-laminar layer resistances (r_a and r_b ,
123 respectively) are derived from measured wind speed, friction velocity, and fluxes of sensible and
124 latent heat every half hour using Monin-Obukhov similarity theory (Foken, 2017). The stomatal
125 conductance for O₃ (g_s) is derived from the measured water vapor flux and meteorological data
126 every half hour with the inverted Penman-Monteith equation (Monteith, 1981; Gerosa et al.,
127 2007). Some studies instead calculate g_s from the measured gross primary productivity (GPP)
128 (Lamaud et al., 2009; El-Madany et al., 2017). That method likely underestimates the stomatal
129 flux, however, because the g_s /GPP ratio increases as humidity rises and because g_s remains non-
130 zero when GPP has ceased at night (Dawson et al., 2007; Medlyn et al., 2011). Appendix A
131 provides further details of these calculations. To avoid complications to the Penman-Monteith
132 equation from wet canopies, we exclude times when dew may be present (RH > 80%), and days
133 with precipitation (> 5mm). We also exclude the top and bottom 1% of g_s values, which include
134 many unrealistic outliers (e.g. $|g_s| > 0.5 \text{ m s}^{-1}$). Figure 1 shows the mean stomatal conductance
135 during the growing season (April-September) at all sites.
136

137 The terms in Eqs. 1-3 that cannot be derived from FLUXNET2015 measurements are O₃ mole
138 fraction and non-stomatal conductance. The O₃ mole fraction is taken from a gridded dataset of
139 hourly O₃ measurements that spans the contiguous United States and Europe (Schnell et al.,
140 2014). This dataset has 1° spatial resolution, so some differences from measured O₃ abundances
141 at individual sites are inevitable. Schnell et al. (2014) estimated these errors to be 6-9 ppb (rms)
142 or about 15% of summer mean O₃ in the US and similar in Europe. Figure 2 shows that the
143 daytime gridded O₃ concentrations correlate well with observations at three flux tower sites
144 where O₃ was measured ($R^2 = 0.63\text{-}0.87$) and have modest negative bias (5-10 ppb, -12 to -
145 28%), consistent with the accuracy reported by Schnell et al. (2014). We use the Zhang et al.
146 (2003) parameterization of non-stomatal conductance, which accounts for O₃ deposition to leaf
147 cuticles and ground and has been evaluated at sites in North America. The parameterization
148 requires leaf-area index, which we take from satellite remote sensing (Claverie et al., 2014;
149 2016), snow depth, which we take from MERRA2 reanalysis (GMAO, 2015; Gelaro et al.,
150 2017), and standard meteorological data provided by FLUXNET2015.
151

152 Figure 3 shows the stomatal O₃ flux at each site calculated with Eq. 3, then averaged over the
153 April-September growing season. Figure S1 shows the corresponding total O₃ flux (Eq. 1). We
154 refer to these products as the “synthetic” total and stomatal O₃ fluxes (F'_{O_3} and F'_{s,O_3} ,
155 respectively) and use a prime to distinguish them from the measured O₃ fluxes (F_{O_3} and F_{s,O_3})
156 that are only available at a few sites. Together, we refer to F'_{O_3} and F'_{s,O_3} as SynFlux. In total, the
157 measurements required to calculate F'_{s,O_3} are O₃ mole fraction, sensible and latent heat fluxes,
158 friction velocity, temperature, pressure, humidity, canopy height, and leaf area index. There are
159 43 sites in the US and 60 sites in Europe within the FLUXNET Tier 1 database with sufficient
160 measurements to calculate F'_{s,O_3} .



161

162

163 **2.2 Observed O₃ flux**

164

165 We evaluate SynFlux and its inputs at three sites where O₃ flux measurements are available:
166 Harvard Forest, Massachusetts, United States (Munger et al., 1996); Blodgett Forest, California,
167 United States (Fares et al., 2010); and Hyytiälä Forest, Finland (Keronen et al., 2003;
168 Mammarella et al., 2007; Rannik et al., 2009). These forest sites sample a range of
169 environmental and ecosystem conditions summarized in Table 1. All three sites have at least 6
170 years of half-hourly or hourly flux measurements. Two sites are evergreen needleleaf forests
171 (Blodgett and Hyytiälä), while one is a deciduous broadleaf forest containing some scattered
172 stands of evergreen needleleaf trees (Harvard). Climate also differs across these sites. Blodgett
173 Forest has a Mediterranean climate with cool, wet winters and hot, dry summers. Hyytiälä and
174 Harvard Forests have cold winters and wetter summers, with Harvard Forest being the warmer of
175 the two.

176

177 Harvard Forest water vapor flux measurements were recalibrated for this work based on
178 matching water vapor mixing ratio measured by the flux sensor to levels calculated from ambient
179 relative humidity and air temperature, resulting in a 30% increase in evapotranspiration during
180 the 1990s and no change since 2006. In addition, we remove sub-canopy evaporation from the
181 measured water vapor flux before the Penman-Monteith calculation. Based on past
182 measurements at these sites, the sub-canopy fraction of evapotranspiration is 20% at Hyytiälä
183 Forest, 10% at Harvard Forest in summer, and 50% at Harvard Forest in months without leaves
184 (Moore et al., 1996; Launiainen et al., 2005). We are unable to make this correction at all
185 FLUXNET sites since water vapor flux is typically measured only above canopy.

186

187 At these three sites, observed v_d , g_{ns} , and F_{s,O_3} can be derived from the F_{O_3} measurements with
188 methods that differ slightly from Sect. 2.1. O₃ deposition velocity is inferred from measurements
189 of O₃ concentration and flux via $v_d = F_{O_3}(n\chi)^{-1}$. Resistance or conductance terms r_a , r_b , and g_s
190 are calculated as described in Sect. 2.1, then both canopy and non-stomatal conductance are
191 derived from observations via $g_c = (v_d^{-1} - r_a - r_b)^{-1}$ and $g_{ns} = g_c - g_s$, respectively. With
192 those values, Eq. 3 gives the observed stomatal O₃ flux. The half-hourly or hourly measured and
193 synthetic flux still have some outliers (Fig. S2), but the error analysis reveals that most of the
194 outlying points have large uncertainties.

195

196

197 **2.3 Gap filling for friction velocity**

198

199 The FLUXNET2015 dataset uses gap filling for most flux and meteorological measurements
200 (Vuichard and Papale, 2015), but not for friction velocity (u_*), which is required to calculate v_d



201 and F'_{s,O_3} . Filling this one variable would significantly reduce the fraction of missing data in our
202 analysis. Monin-Obukhov similarity theory predicts that friction velocity is proportional to wind
203 speed in the surface layer, for a given roughness length and stability regime (Foken, 2017). On
204 this basis, we regress the available friction velocity measurements against wind speed and net
205 radiation (a proxy for stability) separately for each site and month (a proxy for vegetation
206 roughness). This gap filling was possible at 91 sites that report net radiation measurements.
207

208 The predicted friction velocities from the regression model are highly correlated with available
209 observations ($R^2 > 0.7$) and have minimal mean bias ($\pm 10\%$) at 68 out of 91 eligible sites (Fig.
210 S3). At the remaining 23 sites, frequent stagnant and stable conditions ($u_* \lesssim 0.5 \text{ m s}^{-1}$) degrade
211 the regression performance. We used the regression model to fill missing friction velocity
212 measurements and were thus able to increase the number of F'_{s,O_3} estimates by 1-20%. The
213 differences between monthly mean F'_{s,O_3} with and without gap filling are 10% (rms), so although
214 the u_* gap filling is a potential source of uncertainty, the F'_{s,O_3} estimates are robust.
215

216 2.4 Error analysis, averaging, and numerical methods

217
218 We quantify the errors in F'_{O_3} , F'_{s,O_3} , and all other calculated variables from the measurement
219 uncertainties using standard techniques for propagation of errors through all equations (see
220 Appendix B). This method provides the uncertainty, quantified as standard deviation, of each
221 variable in each half hour interval. The error analysis reveals that F'_{s,O_3} and other derived
222 quantities have uncertainties that change from hour to hour by two orders of magnitude (Fig. S2).
223 In addition, many extreme values of F'_{s,O_3} , g_s , and other variables have very large uncertainties.
224 We retain these outliers in our analysis and use the error analysis to appropriately reduce their
225 influence on averages and other statistics, as described below, without discarding data.
226

227 The FLUXNET2015 dataset contains error estimates for sensible and latent heat measurements.
228 We use these reported values in the error analysis. Where uncertainties in these fluxes are
229 missing, we fill the gaps using a linear regression of available flux errors against flux values for
230 that site. For friction velocity, the uncertainty is the prediction error in the linear model used for
231 gap filling (Sect. 2.3). Based on expert judgment, the standard deviation of O₃ mole fraction is
232 set to 20%, pressure to 0.5 hPa, temperature to 0.5 K, relative humidity to 5%, and canopy height
233 to the lesser of 15% or 2 m. For leaf area index, we use reported uncertainties in the remote
234 sensing for each plant functional type (Claverie et al., 2013; 2016). The Zhang et al. (2003) g_{ns}
235 parameterization has 5 vegetation-specific parameters and all are assigned 50% standard
236 deviation. Zero error is assumed for the flux tower height. Based on these inputs, the median
237 relative uncertainty in F'_{s,O_3} is 44%, but it rises to several hundred percent for some half-hour
238 intervals. The error analysis shows that most of the uncertainty in F'_{s,O_3} derives from uncertainty
239 in the latent heat flux measurement.



240

241 Daily and monthly averages of F'_{s,O_3} and other quantities are constructed in stages. We first
242 calculate a mean diurnal cycle for the day or month by pooling measurements during each hour
243 in a maximum likelihood estimate, a weighted average that accounts for the uncertainty in each
244 measurement. The maximum likelihood estimate is appropriate when combining values from the
245 same distribution, which is expected to apply for measurements within a particular hour, but not
246 across hours of the day. We then average across hours with an unweighted mean to calculate the
247 daily or monthly value. Seasonal values are the unweighted mean of the months they contain.
248 Uncertainties are propagated through each stage of these averages, as detailed in Appendix B.
249 Our discussion focuses on daily averages of daytime data when the sun is at least 4° above the
250 horizon.

251 Analyses are performed in Python 3.5 with NumPy, Pandas, PySolar, and Statsmodels (Reda and
252 Andreas, 2005; Van Der Walt et al., 2006; McKinney, 2010; Seabold et al., 2010). We quantify
253 the slope and strength of linear relationships between variables using standard major axis fitting
254 (SMA, Warton et al., 2006), the non-parametric Thiel-Sen slope (Sen, 1968), and coefficient of
255 determination (R^2).

256

257 2.5 Data availability

258

259 The SynFlux dataset produced in this work is available in the supplementary information for
260 download and use. The dataset includes synthetic stomatal and total O₃ fluxes, O₃ concentrations,
261 O₃ deposition velocity, canopy conductance, stomatal conductance, and all of their propagated
262 uncertainties. Monthly mean values are provided, with and without u_* gap filling, for 103 sites
263 totaling 926 site-years.

264

265

266 3 Results and discussion

267

268 3.1 Evaluation of synthetic fluxes

269

270 Figure 4 compares daily daytime averages of synthetic F'_{s,O_3} to measured F_{s,O_3} . At all three sites,
271 F'_{s,O_3} is strongly correlated with measured values ($R^2 = 0.83\text{--}0.93$). The mean and median biases
272 are -16 to -21% and at least 95% of F'_{s,O_3} values agree with measurements within a factor of 2.
273 The majority of F'_{s,O_3} values lie near the 1:1 line with F_{s,O_3} and the slopes (0.71 to 0.85) reflect
274 this. For 98% of points, the differences between F'_{s,O_3} and F_{s,O_3} are less than the 95% confidence
275 interval derived from the error analysis (two-sided t test). Thus, the errors in F'_{s,O_3} are consistent
276 with the uncertainty in the observations. The half hourly F'_{s,O_3} values perform similarly well
277 against observations (Fig. S4), but our analysis focuses on averages. Overall, these results



278 suggest that synthetic F'_{s,O_3} is a reliable estimate of stomatal O₃ uptake into plants that can be
279 used at eddy covariance sites without O₃ measurements.
280
281 The measurements enable us to evaluate synthetic total deposition, F'_{O_3} , as well, although this is
282 less relevant to ecosystem impacts than stomatal uptake, F'_{s,O_3} . Figure S5 shows that bias (-13 to
283 +65%), slope (0.3-1.4), and R^2 (0.05-0.43) for F'_{O_3} are all worse than for F'_{s,O_3} . The reasons can
284 be derived from Eq. 3. The canopy resistance for O₃ is normally much greater than the quasi-
285 laminar layer and aerodynamic resistances, meaning $r_c \gg r_a$ and $r_c \gg r_b$, often by a factor of 3-
286 10. Therefore, the O₃ deposition velocity is approximately $v_d \approx r_c^{-1} = g_c$. Under these
287 conditions, Eq. 1 simplifies to $F_{O_3} \approx n\chi(g_s + g_{ns})$ and Eq. 3 simplifies to $F_{s,O_3} \approx n\chi g_s$. While
288 g_s is calculated from measured H₂O fluxes, g_{ns} comes from a parameterization, which inevitably
289 introduces error into g_{ns} and F'_{O_3} . Since F'_{s,O_3} has little sensitivity to g_{ns} or its errors, it can be
290 calculated more accurately than F'_{O_3} , as seen when comparing Figures 4 and S4. Despite these
291 larger errors, the F'_{O_3} mean is within 50% of the observed value at two sites and within a factor of
292 2 at all, which may be useful for some applications, given the paucity of prior F_{O_3} measurements.
293
294

295 3.2 Stomatal and non-stomatal deposition

296

297 Figure 5 shows the seasonal cycles of observed O₃ deposition velocity and its important
298 components at the three study sites with O₃ flux measurements. For low or moderately reactive
299 gases like O₃, canopy resistance is typically greater than aerodynamic or quasi-laminar layer
300 resistance, so it controls the overall deposition velocity. At these three sites, deposition velocity
301 is lowest in winter (0.1-0.2 cm s⁻¹) and highest in summer (0.5–0.6 cm s⁻¹). Stomatal
302 conductance, which peaks when weather conditions favor growth, explains most of this seasonal
303 variation, except at Blodgett Forest as discussed below. Stomatal conductance is generally
304 thought to exceed non-stomatal conductance during the growing season at most vegetated sites
305 (Wesely, 1989; Zhang et al., 2003). At both Harvard and Hyttiälä Forests, the mean stomatal
306 conductance (0.2-0.6 cm s⁻¹) is 1.5-6 times larger than non-stomatal conductance (0.08-0.2 cm s⁻¹)
307 during the growing season, so about 60-90% of O₃ deposition occurs through stomatal uptake.
308 In winter at these sites, the calculated stomatal conductance can exceed canopy conductance,
309 which is not possible, but is likely an artifact of evaporation from soil or snow exceeding leaf
310 transpiration at that time of year. At Blodgett, non-stomatal conductance slightly exceeds
311 stomatal conductance in summer (0.4 vs. 0.3 cm s⁻¹). The fast non-stomatal deposition is
312 explained by O₃ reacting with biogenic terpenoid emissions below the flux measurement height
313 (Kurpius and Goldstein, 2003; Fares et al., 2010). These biogenic emissions depend strongly on
314 temperature and light and have a large seasonal cycle with maxima in summer and minima in
315 winter, so stomatal uptake is generally < 50% of O₃ deposition at Blodgett in the summer but >
316 70% in winter.



317

318 A recent analysis of O₃ flux measurements at Harvard Forest suggests that non-stomatal
319 deposition averages 40% of daytime O₃ deposition during summer months, with a range of 10-
320 60% across years (Clifton et al., 2017). Our analysis of the same site, using re-calibrated latent
321 heat flux measurements, does not support such a large role for non-stomatal deposition at this
322 site in summer. As seen in Fig. 5, only 15% of O₃ deposition is non-stomatal during these
323 months, with a range of 4-32% across years. At Hyytiälä Forest, our results are consistent with
324 prior work that found that the non-stomatal deposition is 26% to 44% of daytime O₃ deposition
325 during the growing season (Rannik et al., 2012). Nevertheless, non-stomatal deposition equals or
326 exceeds stomatal uptake where there are large terpene emissions (e.g. Blodgett) and at some
327 other temperate sites that probably lack large biogenic emissions (Fowler et al., 2001; Cieslik,
328 2004; Lamaud et al., 2009; Stella et al., 2011; El-Madany et al., 2017).

329

330 At Harvard and Hyytiälä Forests, the parameterized g_{ns} has a similar mean to measurements
331 during summer, with discrepancies less than a factor of two (Fig. 5). The observed day-to-day
332 variability in g_{ns} is as large as the variability in g_s at Harvard and Hyytiälä Forests and the
333 calculated g_{ns} does not reproduce it ($R^2 < 0.09$), so an important but undetermined non-stomatal
334 process is missing from the parameterization. At Blodgett Forest, the parameterized g_{ns} is one-
335 third of measured g_{ns} in summer, but this is not surprising since the parameterization does not
336 account for O₃ reactions with biogenic volatile organic compounds (BVOC), which are known to
337 be important at this site (Fares et al., 2010). We attempted, unsuccessfully, to use BVOC
338 emissions from the MEGAN biogenic emission model (Guenther et al., 2012) to improve the g_{ns}
339 parameterization, but the correlations between measured g_{ns} and compounds that react fastest
340 with O₃ (monoterpenes and sesquiterpenes) were poor ($R^2 \leq 0.15$). On that basis, synthetic F'_{O₃}
341 may also underestimate total O₃ deposition at other sites with high monoterpene and
342 sesquiterpene emissions, such as warm-weather pine forests, but synthetic F'_{s,O₃} should retain its
343 quality everywhere.

344

345

346 3.3 Spatial patterns of synthetic fluxes

347

348 Across the 43 sites in the US shown in Fig. 3, mean F'_{s,O₃} during the growing season ranges from
349 0.5 to 11.0 nmol m⁻² s⁻¹ with an average of 4.4 nmol m⁻² s⁻¹. The highest F'_{s,O₃} generally occurs in
350 the Midwest (5-9 nmol m⁻² s⁻¹ in Wisconsin, Michigan, Nebraska, Ohio) due to its moderate O₃
351 concentrations (Fig. S6) and moisture levels, which promotes stomatal conductance (Fig. 1). The
352 Western US has higher average O₃ concentrations, but generally lower moisture and stomatal
353 conductance, especially the Southwest US, so F'_{s,O₃} (0-4 nmol m⁻² s⁻¹) is mostly lower than the
354 Midwest. Land cover, land management, and plant types drive large differences in F'_{s,O₃} between
355 nearby sites, even when O₃ concentrations and meteorology are similar. For example, three



356 Nebraska sites are all crop fields and O₃ concentrations are nearly identical, but two irrigated
357 fields have higher stomatal conductance and higher F'_{s,O_3} than the nearby rainfed field (6.2 vs.
358 4.8 nmol m⁻² s⁻¹). Two sites in central California have high g_s and F'_{s,O_3} compared to surrounding
359 sites due to irrigation and naturally wet soil in the California Delta. A combination of topography
360 and climate is also an important factor in California: forest sites in the Sierra Nevada mountains
361 have lower g_s and F'_{s,O_3} than the lowland crops and wetland grasses. In Oregon, an evergreen
362 needleleaf site regrowing after a fire has higher g_s and F'_{s,O_3} than two older forest stands nearby.
363 The differences between 9 Wisconsin forest sites, however, are mostly due to different years of
364 data at each site combined with interannual variability in F'_{s,O_3} ; fluxes at these sites are similar in
365 overlapping years.
366

367 Variability across the 60 sites in Europe is controlled by similar factors. Stomatal uptake ranges
368 from 1.4 to 9.6 nmol m⁻² s⁻¹, with an average of 4.7 nmol m⁻² s⁻¹ (Fig. 3). The Mediterranean
369 region has high O₃ concentrations (Fig. S6), but generally low stomatal conductance due to the
370 dry climate (Fig. 1). Within this region, vegetation type explains broad patterns. Shrub sites in
371 Spain, France, and Sardinia have very low g_s (~0.15 cm s⁻¹) so F'_{s,O_3} is low (1-3 nmol m⁻² s⁻¹),
372 while the most of the sites in mainland Italy are broadleaf and evergreen forests that have slightly
373 greater g_s (~0.2-0.4 cm s⁻¹) and F'_{s,O_3} (3-6 nmol m⁻² s⁻¹), despite similar climate and O₃. In
374 central and northern Europe, temperate climate promotes higher stomatal conductance while O₃
375 concentrations remain modest throughout the growing season. The largest F'_{s,O_3} is 9.8 nmol m⁻² s⁻¹
376 ¹ at a deciduous broadleaf forest in Switzerland, while nearby evergreen forests, cereal crops, and
377 grasslands all have lower fluxes (6-8 nmol m⁻² s⁻¹). While Finland has generally low F'_{s,O_3} of 2-5
378 nmol m⁻² s⁻¹, the high end of this range is similar to rural sites in Germany, illustrating that O₃
379 can impact ecosystems with low O₃ concentrations far from major industrial emissions.
380

381 Table 2 quantifies SynFlux, O₃ deposition velocity, and conductance for each plant functional
382 type. Wetlands, crops, and forests have the highest average F'_{s,O_3} , which is about two times
383 higher than woody savanna or shrublands, the vegetation types with the lowest F'_{s,O_3} . The
384 vegetation types rank in the same order for stomatal conductance, again showing stomata as the
385 main control on O₃ deposition and uptake. Stomatal uptake exceeds non-stomatal uptake for all
386 plant functional types except woody savanna and shrubland. O₃ deposition velocities reported in
387 the table fall within the ranges of past literature, as reviewed by Silva and Heald (2017).
388 However, while Silva and Heald found that the mean deposition velocity was greater over
389 deciduous forests than coniferous forests, crops, or grass, we do not. Rather, we find that
390 variability between sites within each of these categories is large, having a standard deviation
391 about 30% of the multi-site mean.
392

393 3.4 Metrics for O₃ damage to plants 394



395 Since O₃ injures plants mainly by internal oxidative damage after entering the leaves through
396 stomata, the most physiological predictor of plant injuries is the cumulative uptake of O₃ (CUO,
397 Reich, 1987; Fuhrer, 2000; Karlsson et al., 2004; Cieslik, 2004; Matyssek et al., 2007). CUO is
398 defined as the cumulative stomatal O₃ flux exceeding a threshold flux Y that can be detoxified by
399 the plant, integrated over a period of time:

400
$$\text{CUOY} = \sum_i H(F_{s,O_3,i} - Y)(F_{s,O_3,i} - Y) \Delta t_i.$$

401 Here, $H(x)$ is the Heaviside step function and Δt_i is the time elapsed during measurement of
402 $F_{s,O_3,i}$. The sum is carried out over time i in the growing season, which we take to be April to
403 September. The detoxification threshold varies across vegetation types, even among related
404 species (Karlsson et al., 2004, Büker et al., 2015), and thresholds for specific FLUXNET sites
405 are generally unknown. As a compromise, we calculate CUO, with Y=0, and also CUO3, with Y
406 = 3 nmol m⁻² s⁻¹, which has been suggested as a reasonable generic threshold (Mills et al., 2011).
407 CUO is always greater than CUO3, but the sites with high CUO tend to also have high CUO3, so
408 their spatial patterns are similar (Fig. S7).

409
410 While CUO is a physiological dose, concentration-based metrics remain common for assessing
411 ozone impacts because they are easier to measure. Concentration-based metrics quantify O₃ in
412 ambient air irrespective of whether that O₃ enters leaves. These metrics follow the general form

413
$$M = \sum_i w(\chi_i) (\chi_i - \chi_c) \Delta t_i$$

414 where $w(\chi)$ is a weighting function applied to the O₃ mole fraction χ , and χ_c is a constant. Like
415 CUO, the sum is usually over time i during the growing season. Three of the most common
416 concentration-based O₃ metrics are the mean O₃ concentration, the accumulated concentration
417 over a threshold of 40 ppb (AOT40; UNECE, 2004), and the sigmoidal-weighted index (W126;
418 Lefohn and Runeckles, 1987). For mean, $w(\chi) = (\sum \Delta t_i)^{-1}$ and $\chi_c = 0$. For AOT40, $w(\chi) =$
419 $H(\chi - \chi_c)$ and $\chi_c = 40$ ppb. For W126, $w(\chi) = (1 + 4403 \exp(-(126 \text{ ppb}^{-1})\chi))^{-1}$ and $\chi_c =$
420 0. Both AOT40 and W126 use only daytime (8am-8pm) measurements and W126 also takes the
421 maximum value over a 3-month period. The weighting functions for AOT40 and W126 give
422 little or no weight to O₃ concentrations below 40 ppb. In addition, W126 gives increasing weight
423 to concentrations up to about 110 ppb and full weight for higher concentrations based on the
424 understanding that exposure to high O₃ concentrations is more injurious than moderate or low
425 concentrations. Other concentration-based metrics (e.g. SUM60) use other thresholds or
426 weighting functions, but many are strongly correlated with AOT40 or W126 or otherwise
427 qualitatively similar (Paoletti et al., 2007).

428
429 The spatial patterns of AOT40 and W126 closely resemble that of mean O₃ concentration in the
430 US and Europe despite their different weighting functions (Fig. S7). The CUO and CUO3 spatial
431 patterns, however, are similar to F'_{s,O_3} and distinct from the concentration-based metrics. This



432 illustrates that locations with high AOT40 or W126, like the Southwest US or Mediterranean
433 Europe, can have low CUO.
434
435 Even though concentration-based metrics do not measure the physiological O₃ dose to plants,
436 they can be useful if the metric is proportional to the flux-based dose and injuries. Indeed, many
437 controlled experiments and observational studies have documented correlations between both
438 AOT40 and W126 and either uptake or plant injuries (e.g. Fuhrer et al., 1997; Cieslik, 2004;
439 Musselman et al., 2006; Matyssek et al., 2010). However, many of these studies were carried out
440 at a single site or under conditions where stomatal conductance was relatively steady while O₃
441 concentrations varied, for example by maintaining well-watered soil. When stomatal
442 conductance varies widely, such as between arid and humid climates or seasons, concentration-
443 based metrics may not correlate with stomatal O₃ flux (Mills et al., 2011).
444
445 Figure 6 shows that all of the concentration-based metrics are poorly correlated with CUO across
446 the sites (AOT40: $R^2 = 0.05$, W126: $R^2 = 0.03$, mean O₃: $R^2 = 0.04$). Humidity helps explain some
447 of the scatter in Figure 6. The sites with high concentration-based metrics and low CUO have
448 high vapor pressure deficit (VPD), low stomatal conductance, and are mostly in the western US
449 and Mediterranean Europe. Restricting the analysis to humid sites ($VPD < 1.5 \text{ kPa}$) does not
450 improve the correlation ($R^2 \approx 0.05$) and at the arid sites ($VPD > 1.6 \text{ kPa}$) the concentration-based
451 metrics are modestly anti-correlated with CUO (AOT40: $R^2 = 0.19$, W126: $R^2 = 0.05$, mean O₃:
452 $R^2 = 0.37$). This result reinforces that concentration-based metrics can misrepresent CUO and
453 plant injuries (Mills et al., 2011).
454
455 From the CUO values in Table 2, we can estimate the range of O₃ impacts on biomass
456 production at the FLUXNET sites. Although species vary in their sensitivity to O₃, several
457 studies suggest that the biomass production of broadleaf and needleleaf trees decreases 0.2 to 1%
458 per mmol m⁻² of CUO (Karlsson et al., 2004; Wittig et al., 2007; Hoshika et al., 2015).
459 Combining the mean CUO for each plant functional type (Table 2) with these sensitivities, our
460 work implies that O₃ reduces the biomass production at these FLUXNET sites by 6-29% for
461 deciduous broadleaf forests and 4-20% for needleleaf forests. The range represents the spread of
462 reported dose-response sensitivities within each plant type, meaning the least and most O₃-
463 sensitive species. Lombardozzi et al. (2013) caution that species-specific responses to O₃ may
464 not generalize to plant functional types, but the biomass reductions calculated here still indicate
465 the general magnitude of expected O₃ damages. Several broadleaf crops are more sensitive to O₃,
466 with biomass reductions of 1.3-1.6% per mmol m⁻² of CUO (Mills et al., 2011). That sensitivity
467 implies 20-24% drop in biomass production at FLUXNET crop sites. Some studies have
468 quantified O₃ dose-response relationships with other thresholds Y = 1.6 to 6 nmol m⁻² s⁻¹ (e.g.
469 Karlsson et al., 2007; Pleijel et al., 2004, 2014), but the sensitivities have similar magnitude.
470 Fares et al. (2013) also demonstrated 12-19% reduction in gross primary production due to O₃ at
471 some of the same crop and forest FLUXNET sites. Using prognostic models of O₃



472 concentrations and stomatal uptake, several past studies have also suggested that O₃ reduces
473 biomass production and CO₂ sequestration by 4-20% in the US and Europe (Sitch et al., 2007;
474 Wittig et al., 2007; Mills et al., 2011; Yue et al., 2014, 2016; Lombardozzi et al., 2015). Our
475 results support this range of impacts, although some FLUXNET sites and species likely
476 experience greater O₃ injury, but here the CUO is highly constrained from observations and
477 therefore avoids the additional uncertainties of atmosphere-biosphere models.

478

479

480 4 Conclusions

481

482 We have demonstrated a method to estimate O₃ fluxes and stomatal O₃ uptake at eddy
483 covariance flux towers wherever regional O₃ monitors exist. The method, called SynFlux,
484 derives stomatal conductance and O₃ deposition velocity from standard eddy covariance
485 measurements and combines them with gridded O₃ concentrations from air quality monitoring
486 networks. We apply this method to the FLUXNET2015 dataset and derive synthetic flux
487 estimates at 43 sites in the United States and 60 sites in Europe, totaling 926 site-years of
488 observations. O₃ deposition measurements have previously only been sporadically available for a
489 few sites around the world, so this work dramatically increases the flux data available for
490 understanding O₃ impacts on vegetation and for evaluating air quality and climate models.

491

492 Three sites with long-term O₃ flux measurements provide an independent test of SynFlux. These
493 comparisons show that daily averages of synthetic stomatal F'_{s,O_3} correlate well with measured
494 F_{s,O_3} ($R^2 = 0.83\text{-}0.93$) and have a mean bias under 22% at all sites. At all three sites 95% of the
495 synthetic F'_{s,O_3} values differ from measurements by a factor of 2 or less. The differences between
496 F'_{s,O_3} and F_{s,O_3} are also consistent with propagated uncertainty in the underlying measurements.
497 Synthetic total deposition, F'_{O_3} , is sensitive to errors in the parameterized non-stomatal
498 conductance, but mean values are still within a factor of 2 of observations. The errors in this
499 dataset are modest compared with differences between observations and regional and global
500 atmospheric chemistry models that are frequently a factor of 2 or more (Zhang et al., 2003;
501 Hardacre et al., 2015; Clifton et al., 2017; Silva and Heald, 2017), illustrating the utility of this
502 dataset for evaluating models and O₃ impacts.

503

504 Across flux tower sites in the US and Europe, F'_{s,O_3} ranges from 0.5 to 11.0 nmol m⁻² s⁻¹ during
505 the summer growing season. The spatial pattern of F'_{s,O_3} is mainly controlled by stomatal
506 conductance rather than O₃ concentration. Patterns of stomatal conductance and F'_{s,O_3} in turn are
507 explained by climate, especially atmospheric and soil moisture, vegetation types, and land
508 management, such as irrigation. O₃ concentration-based metrics (AOT40, W126, mean O₃) have
509 been widely used to evaluate O₃ damages to plants because they are easier and cheaper to
510 measure than the cumulative uptake of O₃ (CUO) into leaves. However, these metrics have very



511 little correlation with CUO ($R^2 \leq 0.05$) across FLUXNET sites. Using dose-response
512 relationships between CUO and biomass reduction, we estimate that O₃ reduces biomass
513 production and carbon uptake by 4-29%, depending on the site and plant type. Unlike most past
514 estimates, which have used prognostic models of O₃ uptake, our assessment of biomass reduction
515 is based on O₃ fluxes that are tightly constrained by observations. To promote further
516 applications in ecosystem monitoring and modeling, the SynFlux dataset is publicly available in
517 the supplement as monthly averages of F'_{s,O_3} , F'_{O_3} , O₃ deposition velocity, stomatal conductance,
518 and related variables.
519
520
521

522 Acknowledgments

523 This work was supported by the Winchester Fund and by the Council on Research Creativity at
524 Florida State University. Eddy covariance data used here were acquired and shared by the
525 FLUXNET community, including the AmeriFlux and CarboEuropeIP networks. The FLUXNET
526 eddy covariance data processing and harmonization was carried out by the European Fluxes
527 Database Cluster, AmeriFlux Management Project, and Fluxdata project of FLUXNET, with the
528 support of CDIAC and ICOS Ecosystem Thematic Center, and the OzFlux, ChinaFlux and
529 AsiaFlux offices. TFK was supported by the Director, Office of Science, Office of Biological
530 and Environmental Research of the US Department of Energy under Contract DE-AC02-
531 05CH11231 as part of the RUBISCO SFA. The O₃ concentration and flux measurements from
532 Harvard Forest used in this analysis were supported by the National Science Foundation through
533 the LTER program and various programs under the U. S. Department of Energy Office of
534 Science (BER). At Hyytiälä Forest, O₃ concentrations and flux measurements were supported by
535 ICOS-Finland (281255) and Academy of Finland Center of Excellence programme (307331). At
536 Blodgett Forest, O₃ concentrations and flux measurements were supported by ICOS-Finland
537 (281255) and Academy of Finland Center of Excellence programme (307331). The long term O₃
538 concentration and flux measurements from Blodgett Forest used in this analysis were supported
539 by a combination of grants from the Kearney Foundation of Soil Science, the University of
540 California Agricultural Experiment Station, and the U.S. Department of Energy Office of
541 Science (BER), the National Science Foundation Atmospheric Chemistry Program, and the
542 California Air Resources Board.
543



544 **References**

545

546 Acosta, M., Pavelka, M., Montagnani, L., Kutsch, W., Lindroth, A., Juszczak, R. and Janouš, D.:
547 Soil surface CO₂ efflux measurements in Norway spruce forests: Comparison between four
548 different sites across Europe — from boreal to alpine forest, *Geoderma*, 192, 295–303,
549 doi:10.1016/j.geoderma.2012.08.027, 2013.

550

551 Ainsworth, E. A. and Long, S. P.: What have we learned from 15 years of free-air CO₂
552 enrichment (FACE)? A meta-analytic review of the responses of photosynthesis, canopy
553 properties and plant production to rising CO₂, *New Phytol.*, 165(2), 351–372,
554 doi:10.1111/j.1469-8137.2004.01224.x, 2005.

555

556 Ainsworth, E. E. a, Yendrek, C. R., Sitch, S., Collins, W. J. and Emberson, L. D.: The effects of
557 tropospheric ozone on net primary productivity and implications for climate change., *Annu. Rev.*
558 *Plant Biol.*, 63(March), 637–61, doi:10.1146/annurev-arpplant-042110-103829, 2012.

559

560 Ammann, C., Spirig, C., Leifeld, J. and Neftel, A.: Assessment of the nitrogen and carbon budget
561 of two managed temperate grassland fields, *Agric. Ecosyst. Environ.*, 133(3–4), 150–162,
562 doi:10.1016/j.agee.2009.05.006, 2009.

563

564 Anderson, D. E., Verma, S. B. and Rosenberg, N. J.: Eddy correlation measurements of CO₂,
565 latent heat, and sensible heat fluxes over a crop surface, *Boundary-Layer Meteorol.*, 29(3), 263–
566 272, doi:10.1007/BF00119792, 1984.

567

568 Anthoni, P. M., Knohl, A., Rebmann, C., Freibauer, A., Mund, M., Ziegler, W., Kolle, O. and
569 Schulze, E.-D.: Forest and agricultural land-use-dependent CO₂ exchange in Thuringia,
570 Germany, *Glob. Chang. Biol.*, 10(12), 2005–2019, doi:10.1111/j.1365-2486.2004.00863.x, 2004.
571 Aubinet, M., Chermanne, B., Vandenhaute, M., Longdoz, B., Yernaux, M. and Laitat, E.: Long
572 term carbon dioxide exchange above a mixed forest in the Belgian Ardennes, *Agric. For.*
573 *Meteorol.*, 108(4), 293–315, doi:10.1016/s0168-1923(01)00244-1, 2001.

574

575 Avnery, S., Mauzerall, D. L., Liu, J. and Horowitz, L. W.: Global crop yield reductions due to
576 surface ozone exposure: 1. Year 2000 crop production losses and economic damage, *Atmos.*
577 *Environ.*, 45(13), 2284–2296, doi:10.1016/j.atmosenv.2010.11.045, 2011.

578

579 Baldocchi, D.: AmeriFlux US-Tw4 Twitchell East End Wetland, , doi:10.17190/AMF/1246151,
580 2016.

581

582 Baldocchi, D., Falge, E., Gu, L., Olson, R., Hollinger, D., Running, S., Anthoni, P., Bernhofer,
583 C., Davis, K., Evans, R., Fuentes, J., Goldstein, A., Katul, G., Law, B., Lee, X., Malhi, Y.,
584 Meyers, T., Munger, W., Oechel, W., Paw, U. K. T., Pilegaard, K., Schmid, H. P., Valentini, R.,
585 Verma, S., Vesala, T., Wilson, K. and Wofsy, S.: FLUXNET: A new tool to study the temporal
586 and spatial variability of ecosystem-scale carbon dioxide, water vapor, and energy flux densities,
587 *Bull. Am. Meteorol. Soc.*, 82(11), 2415–2434, doi:10.1175/1520-0477, 2001.

588

589 Baldocchi, D., Chen, Q., Chen, X., Ma, S., Miller, G., Ryu, Y., Xiao, J., Wenk, R. and Battles, J.:



- 590 The dynamics of energy, water, and carbon fluxes in a blue oak (*Quercus douglasii*) savanna in
591 California, *Ecosyst. Funct. Savannas*, 1, 135–151, doi:10.1201/b10275-10, 2010.
592
- 593 Berbigier, P., Bonnefond, J.-M. and Mellmann, P.: CO₂ and water vapour fluxes for 2 years
594 above Euroflux forest site, *Agric. For. Meteorol.*, 108(3), 183–197, doi:10.1016/s0168-
595 1923(01)00240-4, 2001.
596
- 597 Bonan, G. B., Lawrence, P. J., Oleson, K. W., Levis, S., Jung, M., Reichstein, M., Lawrence, D.
598 M. and Swenson, S. C.: Improving canopy processes in the Community Land Model version 4
599 (CLM4) using global flux fields empirically inferred from FLUXNET data, *J. Geophys. Res.*,
600 116(G2), G02014, doi:10.1029/2010JG001593, 2011.
601
- 602 Bowling, D. R., Bethers-Marchetti, S., Lunch, C. K., Grote, E. E. and Belnap, J.: Carbon, water,
603 and energy fluxes in a semiarid cold desert grassland during and following multiyear drought, *J.*
604 *Geophys. Res.*, 115(G4), G04026, doi:10.1029/2010jg001322, 2010.
605
- 606 Büker, P., Feng, Z., Uddling, J., Briolat, A., Alonso, R., Braun, S., Elvira, S., Gerosa, G.,
607 Karlsson, P. E., Le Thiec, D., Marzuoli, R., Mills, G., Oksanen, E., Wieser, G., Wilkinson, M.
608 and Emberson, L. D.: New flux based dose-response relationships for ozone for European forest
609 tree species, *Environ. Pollut.*, 206, 163–174, doi:10.1016/j.envpol.2015.06.033, 2015.
610
- 611 Carrara, A., Janssens, I. A., Yuste, J. C. and Ceulemans, R.: Seasonal changes in photosynthesis,
612 respiration and NEE of a mixed temperate forest, *Agric. For. Meteorol.*, 126(1–2), 15–31,
613 doi:10.1016/j.agrformet.2004.05.002, 2004.
614
- 615 Chiesi, M., Maselli, F., Bindi, M., Fibbi, L., Cherubini, P., Arlotta, E., Tirone, G., Matteucci, G.
616 and Seufert, G.: Modelling carbon budget of Mediterranean forests using ground and remote
617 sensing measurements, *Agric. For. Meteorol.*, 135(1–4), 22–34,
618 doi:10.1016/j.agrformet.2005.09.011, 2005.
619
- 620 Cieslik, S. A.: Ozone uptake by various surface types: A comparison between dose and exposure,
621 *Atmos. Environ.*, 38(15), 2409–2420, doi:10.1016/j.atmosenv.2003.10.063, 2004.
622
- 623 Claverie, M., Vermote, E. F., Weiss, M., Baret, F., Hagolle, O. and Demarez, V.: Validation of
624 coarse spatial resolution LAI and FAPAR time series over cropland in southwest France, *Remote
625 Sens. Environ.*, 139, 216–230, doi:10.1016/j.rse.2013.07.027, 2013.
626
- 627 Clifton, O. E., Fiore, A. M., Munger, J. W., Malyshev, S., Horowitz, L. W., Shevliakova, E.,
628 Paulot, F., Murray, L. T. and Griffin, K. L.: Interannual variability in ozone removal by a
629 temperate deciduous forest, *Geophys. Res. Lett.*, 44(1), 542–552, doi:10.1002/2016GL070923,
630 2017.
631
- 632 Cook, B. D., Davis, K. J., Wang, W., Desai, A., Berger, B. W., Teclaw, R. M., Martin, J. G.,
633 Bolstad, P. V., Bakwin, P. S., Yi, C. and Heilman, W.: Carbon exchange and venting anomalies
634 in an upland deciduous forest in northern Wisconsin, USA, *Agric. For. Meteorol.*, 126(3–4),
635 271–295, doi:10.1016/j.agrformet.2004.06.008, 2004.



- 636
637 Delpierre, N., Berveiller, D., Granda, E. and Dufrêne, E.: Wood phenology, not carbon input,
638 controls the interannual variability of wood growth in a temperate oak forest, *New Phytol.*,
639 210(2), 459–470, doi:10.1111/nph.13771, 2015.
640
641 Desai, A. R., Bolstad, P. V, Cook, B. D., Davis, K. J. and Carey, E. V: Comparing net ecosystem
642 exchange of carbon dioxide between an old-growth and mature forest in the upper Midwest,
643 USA, *Agric. For. Meteorol.*, 128(1–2), 33–55, doi:10.1016/j.agrformet.2004.09.005, 2005.
644
645 Desai, A. R., Xu, K., Tian, H., Weishampel, P., Thom, J., Baumann, D., Andrews, A. E., Cook,
646 B. D., King, J. Y. and Kolka, R.: Landscape-level terrestrial methane flux observed from a very
647 tall tower, *Agric. For. Meteorol.*, 201, 61–75, doi:10.1016/j.agrformet.2014.10.017, 2015.
648
649 Dietiker, D., Buchmann, N. and Eugster, W.: Testing the ability of the DNDC model to predict
650 CO₂ and water vapour fluxes of a Swiss cropland site, *Agric. Ecosyst. Environ.*, 139(3), 396–
651 401, doi:10.1016/j.agee.2010.09.002, 2010.
652
653 Van Dingenen, R., Dentener, F. J., Raes, F., Krol, M. C., Emberson, L. and Cofala, J.: The global
654 impact of ozone on agricultural crop yields under current and future air quality legislation,
655 *Atmos. Environ.*, 43(3), 604–618, doi:10.1016/j.atmosenv.2008.10.033, 2009.
656
657 Dolman, A. J., Moors, E. J. and Elbers, J. A.: The carbon uptake of a mid latitude pine forest
658 growing on sandy soil, *Agric. For. Meteorol.*, 111(3), 157–170, doi:10.1016/S0168-
659 1923(02)00024-2, 2002.
660
661 Dragoni, D., Schmid, H. P., Wayson, C. A., Potter, H., Grimmond, C. S. B. and Randolph, J. C.:
662 Evidence of increased net ecosystem productivity associated with a longer vegetated season in a
663 deciduous forest in south-central Indiana, USA, *Glob. Chang. Biol.*, 17(2), 886–897,
664 doi:10.1111/j.1365-2486.2010.02281.x, 2011.
665
666 Dušek, J., Čížková, H., Stellner, S., Czerný, R. and Květ, J.: Fluctuating water table affects gross
667 ecosystem production and gross radiation use efficiency in a sedge-grass marsh, *Hydrobiologia*,
668 692(1), 57–66, doi:10.1007/s10750-012-0998-z, 2012.
669
670 El-Madany, T., Niklasch, K. and Klemm, O.: Stomatal and non-stomatal turbulent deposition
671 flux of ozone to a managed peatland, *Atmosphere (Basel)*, 8(9), 175,
672 doi:10.3390/atmos8090175, 2017.
673
674 Etzold, S., Ruehr, N. K., Zweifel, R., Dobbertin, M., Zingg, A., Pluess, P., Hässler, R., Eugster,
675 W. and Buchmann, N.: The carbon balance of two contrasting mountain forest ecosystems in
676 Switzerland: Similar annual trends, but seasonal differences, *Ecosystems*, 14(8), 1289–1309,
677 doi:10.1007/s10021-011-9481-3, 2011.
678
679 Fares, S., McKay, M., Holzinger, R. and Goldstein, A. H.: Ozone fluxes in a *Pinus ponderosa*
680 ecosystem are dominated by non-stomatal processes: Evidence from long-term continuous
681 measurements, *Agric. For. Meteorol.*, 150(3), 420–431, doi:10.1016/j.agrformet.2010.01.007,



- 682 2010.
683
684 Fares, S., Savi, F., Muller, J., Matteucci, G. and Paoletti, E.: Simultaneous measurements of
685 above and below canopy ozone fluxes help partitioning ozone deposition between its various
686 sinks in a Mediterranean Oak Forest, Agric. For. Meteorol., 198–199, 181–191,
687 doi:10.1016/j.agrformet.2014.08.014, 2014.
688
689 Ferréa, C., Zenone, T., Comolli, R. and Seufert, G.: Estimating heterotrophic and autotrophic soil
690 respiration in a semi-natural forest of Lombardy, Italy, Pedobiologia (Jena), 55(6), 285–294,
691 doi:10.1016/j.pedobi.2012.05.001, 2012.
692
693 Finkelstein, P. L., Ellestad, T. G., Clarke, J. F., Meyers, T. P., Schwede, D. B., Hebert, E. O. and
694 Neal, J. A.: Ozone and sulfur dioxide dry deposition to forests: Observations and model
695 evaluation, J. Geophys. Res. Atmos., 105(D12), 15365–15377, doi:10.1029/2000JD900185,
696 2000.
697
698 Fischer, M. L., Billesbach, D. P., Berry, J. A., Riley, W. J. and Torn, M. S.: Spatiotemporal
699 variations in growing season exchanges of CO₂, H₂O, and sensible heat in agricultural fields of
700 the Southern Great Plains, Earth Interact., 11(17), 1–21, doi:10.1175/ei231.1, 2007.
701
702 Foken, T.: Micrometeorology, 2nd ed., Springer, Berlin, Germany., n.d.
703 Fowler, D., Flechard, C., Cape, J. N., Storeton-West, R. L. and Coyle, M.: Measurements of
704 ozone deposition to vegetation quantifying the flux, the stomatal and non-stomatal components,
705 Water. Air. Soil Pollut., 130(1–4), 63–74, doi:10.1023/A:1012243317471, 2001.
706
707 Frank, J. M., Massman, W. J., Ewers, B. E., Huckaby, L. S. and Negrón, J. F.: Ecosystem
708 CO₂/H₂O fluxes are explained by hydraulically limited gas exchange during tree mortality from
709 spruce bark beetles, J. Geophys. Res. Biogeosciences, 119(6), 1195–1215,
710 doi:10.1002/2013jg002597, 2014.
711
712 Fuhrer, J.: Introduction to the special issue on ozone risk analysis for vegetation in Europe.,
713 Environ. Pollut., 109(3), 359–60 [online] Available from:
714 <http://www.ncbi.nlm.nih.gov/pubmed/15092869>, 2000.
715
716 Fuhrer, J., Skärby, L. and Ashmore, M. R.: Critical levels for ozone effects on vegetation in
717 Europe, Environ. Pollut., 97(1–2), 91–106, doi:10.1016/S0269-7491(97)00067-5, 1997.
718
719 Galvagno, M., Wohlfahrt, G., Cremonese, E., Rossini, M., Colombo, R., Filippa, G., Julitta, T.,
720 Manca, G., Siniscalco, C., di Cella, U. M. and Migliavacca, M.: Phenology and carbon dioxide
721 source/sink strength of a subalpine grassland in response to an exceptionally short snow season,
722 Environ. Res. Lett., 8(2), 25008, doi:10.1088/1748-9326/8/2/025008, 2013.
723
724 Garbulsky, M. F., Penuelas, J., Papale, D. and Filella, I.: Remote estimation of carbon dioxide
725 uptake by a Mediterranean forest, Glob. Chang. Biol., 14(12), 2860–2867, doi:10.1111/j.1365-
726 2486.2008.01684.x, 2008.
727



- 728 Gelaro, R., McCarty, W., Suárez, M. J., Todling, R., Molod, A., Takacs, L., Randles, C. A.,
729 Darmenov, A., Bosilovich, M. G., Reichle, R., Wargan, K., Coy, L., Cullather, R., Draper, C.,
730 Akella, S., Buchard, V., Conaty, A., da Silva, A. M., Gu, W., Kim, G. K., Koster, R., Lucchesi,
731 R., Merkova, D., Nielsen, J. E., Partyka, G., Pawson, S., Putman, W., Rienecker, M., Schubert,
732 S. D., Sienkiewicz, M. and Zhao, B.: The modern-era retrospective analysis for research and
733 applications, version 2 (MERRA-2), *J. Clim.*, 30(14), 5419–5454, doi:10.1175/JCLI-D-16-
734 0758.1, 2017.
- 735
- 736 Gerosa, G., Marzuoli, R., Cieslik, S. and Ballarin-Denti, A.: Stomatal ozone fluxes over a barley
737 field in Italy. “Effective exposure” as a possible link between exposure- and flux-based
738 approaches, *Atmos. Environ.*, 38(15), 2421–2432, doi:10.1016/j.atmosenv.2003.12.040, 2004.
739
- 740 Gerosa, G., Vitale, M., Finco, A., Manes, F., Denti, A. B. and Cieslik, S.: Ozone uptake by an
741 evergreen Mediterranean Forest (*Quercus ilex*) in Italy. Part I: Micrometeorological flux
742 measurements and flux partitioning, *Atmos. Environ.*, 39(18), 3255–3266,
743 doi:10.1016/j.atmosenv.2005.01.056, 2005.
- 744
- 745 Gerosa, G., Derghi, F. and Cieslik, S.: Comparison of different algorithms for stomatal ozone
746 flux determination from micrometeorological measurements, *Water. Air. Soil Pollut.*, 179(1–4),
747 309–321, doi:10.1007/s11270-006-9234-7, 2007.
- 748
- 749 Goldstein, A. H., Hultman, N. E., Fracheboud, J. M., Bauer, M. R., Panek, J. a., Xu, M., Qi, Y.,
750 Guenther, A. B. and Baugh, W.: Effects of climate variability on the carbon dioxide, water, and
751 sensible heat fluxes above a ponderosa pine plantation in the Sierra Nevada (CA), *Agric. For.
752 Meteorol.*, 101(2–3), 113–129, doi:10.1016/S0168-1923(99)00168-9, 2000.
753
- 754 Gough, C. M., Hardiman, B. S., Nave, L. E., Bohrer, G., Maurer, K. D., Vogel, C. S.,
755 Nadelhoffer, K. J. and Curtis, P. S.: Sustained carbon uptake and storage following moderate
756 disturbance in a Great Lakes forest, *Ecol. Appl.*, 23(5), 1202–1215, doi:10.1890/12-1554.1,
757 2013.
- 758
- 759 Grünwald, T. and Bernhofer, C.: A decade of carbon, water and energy flux measurements of an
760 old spruce forest at the Anchor Station Tharandt, *Tellus Ser. B-Chemical Phys. Meteorol.*, 59(3),
761 387–396, doi:10.3402/tellusb.v59i3.17000, 2007.
- 762
- 763 Guidi, L., Nali, C., Lorenzini, G., Filippi, F. and Soldatini, G. F.: Effect of chronic ozone
764 fumigation on the photosynthetic process of poplar clones showing different sensitivity, *Environ.
765 Pollut.*, 113(3), 245–254, doi:10.1016/S0269-7491(00)00194-9, 2001.
- 766
- 767 Hardacre, C., Wild, O. and Emberson, L.: An evaluation of ozone dry deposition in global scale
768 chemistry climate models, *Atmos. Chem. Phys.*, 15(11), 6419–6436, doi:10.5194/acp-15-6419-
769 2015, 2015.
- 770
- 771 Hatala, J. A., Detto, M., Sonnentag, O., Deverel, S. J., Verfaillie, J. and Baldocchi, D. D.:
772 Greenhouse gas (CO₂, CH₄, H₂O) fluxes from drained and flooded agricultural peatlands in the
773 Sacramento-San Joaquin Delta, *Agric. Ecosyst. Environ.*, 150, 1–18,



- 774 doi:10.1016/j.agee.2012.01.009, 2012.
775
776 Holtslag, a. a. M. and De Bruin, H. a. R.: Applied modeling of the nighttime surface energy
777 balance over land, *J. Appl. Meteorol.*, 27(6), 689–704, doi:10.1175/1520-
778 0450(1988)027<0689:AMOTNS>2.0.CO;2, 1988.
779
780 Hommeltenberg, J., Schmid, H. P., Drösler, M. and Werle, P.: Can a bog drained for forestry be
781 a stronger carbon sink than a natural bog forest?, *Biogeosciences*, 11(13), 3477–3493,
782 doi:10.5194/bg-11-3477-2014, 2014.
783
784 Hoshika, Y., Katata, G., Deushi, M., Watanabe, M., Koike, T. and Paoletti, E.: Ozone-induced
785 stomatal sluggishness changes carbon and water balance of temperate deciduous forests, *Sci.
786 Rep.*, 5, 9871, doi:10.1038/srep09871, 2015.
787
788 Imer, D., Merbold, L., Eugster, W. and Buchmann, N.: Temporal and spatial variations of soil
789 CO₂, CH₄ and N₂O fluxes at three differently managed grasslands, *Biogeosciences*, 10(9),
790 5931–5945, doi:10.5194/bg-10-5931-2013, 2013.
791
792 Irvine, J., Law, B. E. and Hibbard, K. A.: Postfire carbon pools and fluxes in semiarid ponderosa
793 pine in Central Oregon, *Glob. Chang. Biol.*, 13(8), 1748–1760, doi:10.1111/j.1365-
794 2486.2007.01368.x, 2007.
795
796 Irvine, J., Law, B. E., Martin, J. G. and Vickers, D.: Interannual variation in soil CO₂ efflux and
797 the response of root respiration to climate and canopy gas exchange in mature ponderosa pine,
798 *Glob. Chang. Biol.*, 14(12), 2848–2859, doi:10.1111/j.1365-2486.2008.01682.x, 2008.
799
800 Jacobs, C. M. J., Jacobs, A. F. G., Bosveld, F. C., Hendriks, D. M. D., Hensen, A., Kroon, P. S.,
801 Moors, E. J., Nol, L., Schrier-Uijl, A. and Veenendaal, E. M.: Variability of annual CO₂
802 exchange from Dutch grasslands, *Biogeosciences*, 4(5), 803–816, doi:10.5194/bg-4-803-2007,
803 2007.
804
805 Jacobson, M. Z.: Fundamentals of atmospheric modeling second edition, Cambridge University
806 Press., 2005.
807
808 Karlsson, P. E., Uddling, J., Braun, S., Broadmeadow, M., Elvira, S., Gimeno, B. S., Le Thiec,
809 D., Oksanen, E., Vandermeiren, K., Wilkinson, M. and Emberson, L.: New critical levels for
810 ozone effects on young trees based on AOT40 and simulated cumulative leaf uptake of ozone,
811 *Atmos. Environ.*, 38(15), 2283–2294, doi:10.1016/j.atmosenv.2004.01.027, 2004.
812
813 Kavassalis, S. C. and Murphy, J. G.: Understanding ozone-meteorology correlations: A role for
814 dry deposition, *Geophys. Res. Lett.*, 44(6), 2922–2931, doi:10.1002/2016GL071791, 2017.
815
816 Keronen, P., Reissell, A., Rannik, Ü., Pohja, T., Siivola, E., Hiltunen, V., Hari, P., Kulmala, M.
817 and Vesala, T.: Ozone flux measurements over a Scots pine forest using eddy covariance
818 method: Performance evaluation and comparison with flux-profile method, *Boreal Environ. Res.*,
819 8(4), 425–443 [online] Available from: <http://www.scopus.com/inward/record.url?eid=2-s2.0->



- 820 0347884158&partnerID=40&md5=4ad114fb52c557d36cc8a0ec1ab8bb7e, 2003.
821
822 Knohl, A., Schulze, E.-D., Kolle, O. and Buchmann, N.: Large carbon uptake by an unmanaged
823 250-year-old deciduous forest in Central Germany, Agric. For. Meteorol., 118(3–4), 151–167,
824 doi:10.1016/s0168-1923(03)00115-1, 2003.
825
826 Knox, S. H., Matthes, J. H., Sturtevant, C., Oikawa, P. Y., Verfaillie, J. and Baldocchi, D.:
827 Biophysical controls on interannual variability in ecosystem-scale CO₂ and CH₄ exchange in a
828 California rice paddy, J. Geophys. Res. Biogeosciences, 121(3), 978–1001,
829 doi:10.1002/2015jg003247, 2016.
830
831 Kurbatova, J., Li, C., Varlagin, A., Xiao, X. and Vygodskaya, N.: Modeling carbon dynamics in
832 two adjacent spruce forests with different soil conditions in Russia, Biogeosciences, 5(4), 969–
833 980, doi:10.5194/bg-5-969-2008, 2008.
834
835 Kurpius, M. R. and Goldstein, A. H.: Gas-phase chemistry dominates O₃ loss to a forest,
836 implying a source of aerosols and hydroxyl radicals to the atmosphere, Geophys. Res. Lett.,
837 30(7), 2–5, doi:10.1029/2002GL016785, 2003.
838
839 Lamaud, E., Loubet, B., Irvine, M., Stella, P., Personne, E. and Cellier, P.: Partitioning of ozone
840 deposition over a developed maize crop between stomatal and non-stomatal uptakes, using eddy-
841 covariance flux measurements and modelling, Agric. For. Meteorol., 149(9), 1385–1396,
842 doi:10.1016/j.agrformet.2009.03.017, 2009.
843
844 Launiainen, S., Rinne, J., Pumpanen, J., Kulmala, L., Kolari, P., Keronen, P., Siivola, E., Pohja,
845 T., Hari, P. and Vesala, T.: Eddy covariance measurements of CO₂ and sensible and latent heat
846 fluxes during a full year in a boreal pine forest trunk-space, Boreal Environ. Res., 10(6), 569–
847 588, 2005.
848
849 Lefohn, A. S. and Runeckles, V. C.: Establishing standards to protect vegetation-ozone
850 exposure/dose considerations, Atmos. Environ., 21(3), 561–568, doi:10.1016/0004-
851 6981(87)90038-2, 1987.
852
853 Lindauer, M., Schmid, H. P., Grote, R., Mauder, M., Steinbrecher, R. and Wolpert, B.: Net
854 ecosystem exchange over a non-cleared wind-throw-disturbed upland spruce forest—
855 Measurements and simulations, Agric. For. Meteorol., 197, 219–234,
856 doi:10.1016/j.agrformet.2014.07.005, 2014.
857
858 Lohila, A.: Annual CO₂ exchange of a peat field growing spring barley or perennial forage grass,
859 J. Geophys. Res., 109, D18116, doi:10.1029/2004jd004715, 2004.
860
861 Lombardozzi, D., Sparks, J. P., Bonan, G. and Levis, S.: Ozone exposure causes a decoupling of
862 conductance and photosynthesis: Implications for the Ball-Berry stomatal conductance model,
863 Oecologia, 169(3), 651–659, doi:10.1007/s00442-011-2242-3, 2012.
864
865 Lombardozzi, D., Sparks, J. P. and Bonan, G.: Integrating O₃ influences on terrestrial processes:



- 866 photosynthetic and stomatal response data available for regional and global modeling,
867 Biogeosciences, 10, 6815–6831, doi:10.5194/bg-10-6815-2013, 2013.
868
869 Lombardozzi, D., Levis, S., Bonan, G., Hess, P. G. and Sparks, J. P.: The influence of chronic
870 ozone exposure on global carbon and water cycles, *J. Clim.*, 28(1), 292–305, doi:10.1175/JCLI-
871 D-14-00223.1, 2015.
872
873 Loubet, B., Laville, P., Lehuger, S., Larmanou, E., Fléchard, C., Mascher, N., Genermont, S.,
874 Roche, R., Ferrara, R. M., Stella, P., Personne, E., Durand, B., Decuq, C., Flura, D., Masson, S.,
875 Fanucci, O., Rampon, J.-N., Siemens, J., Kindler, R., Gabrielle, B., Schrumpf, M. and Cellier, P.:
876 Carbon, nitrogen and Greenhouse gases budgets over a four years crop rotation in northern
877 France, *Plant Soil*, 343(1–2), 109–137, doi:10.1007/s11104-011-0751-9, 2011.
878
879 Ma, S., Baldocchi, D. D., Xu, L. and Hehn, T.: Inter-annual variability in carbon dioxide
880 exchange of an oak/grass savanna and open grassland in California, *Agric. For. Meteorol.*,
881 147(3–4), 157–171, doi:10.1016/j.agrformet.2007.07.008, 2007.
882
883 Mammarella, I., Kolari, P., Rinne, J., Keronen, P., Pumpanen, J. and Vesala, T.: Determining the
884 contribution of vertical advection to the net ecosystem exchange at Hytytälä forest, Finland,
885 *Tellus, Ser. B Chem. Phys. Meteorol.*, 59(5), 900–909, doi:10.1111/j.1600-0889.2007.00306.x,
886 2007.
887
888 Marcolla, B., Pitacco, A. and Cescatti, A.: Canopy architecture and turbulence structure in a
889 coniferous forest, *Boundary-Layer Meteorol.*, 108(1), 39–59, doi:10.1023/a:1023027709805,
890 2003.
891
892 Marcolla, B., Cescatti, A., Manca, G., Zorer, R., Cavagna, M., Fiora, A., Gianelle, D.,
893 Rodeghiero, M., Sottocornola, M. and Zampedri, R.: Climatic controls and ecosystem responses
894 drive the inter-annual variability of the net ecosystem exchange of an alpine meadow, *Agric. For.*
895 *Meteorol.*, 151(9), 1233–1243, doi:10.1016/j.agrformet.2011.04.015, 2011.
896
897 Marrero, T. R. and Mason, E. A.: Gaseous Diffusion Coefficients, *J. Phys. Chem. Ref. Data*,
898 1(1), 3–118, doi:10.1063/1.3253094, 1972.
899
900 Matthes, J. H., Sturtevant, C., Verfaillie, J., Knox, S. and Baldocchi, D.: Parsing the variability in
901 CH4flux at a spatially heterogeneous wetland: Integrating multiple eddy covariance towers with
902 high-resolution flux footprint analysis, *J. Geophys. Res. Biogeosciences*, 119(7), 1322–1339,
903 doi:10.1002/2014jg002642, 2014.
904
905 Matyssek, R., Bahnweg, G., Ceulemans, R., Fabian, P., Grill, D., Hanke, D. E., Kraigher, H.,
906 Oßwald, W., Rennenberg, H., Sandermann, H., Tausz, M. and Wieser, G.: Synopsis of the
907 CASIROZ case study: Carbon sink strength of *Fagus sylvatica* L. in a changing environment -
908 Experimental risk assessment of mitigation by chronic ozone impact, *Plant Biol.*, 9(2), 163–180,
909 doi:10.1055/s-2007-964883, 2007.
910
911 Matyssek, R., Karnosky, D. F., Wieser, G., Percy, K., Oksanen, E., Grams, T. E. E., Kubiske,



- 912 M., Hanke, D. and Pretzsch, H.: Advances in understanding ozone impact on forest trees:
913 Messages from novel phytotron and free-air fumigation studies, *Environ. Pollut.*, 158(6), 1990–
914 2006, doi:10.1016/j.envpol.2009.11.033, 2010.
915
- 916 Mauder, M., Cuntz, M., Drüe, C., Graf, A., Rebmann, C., Schmid, H. P., Schmidt, M. and
917 Steinbrecher, R.: A strategy for quality and uncertainty assessment of long-term eddy-covariance
918 measurements, *Agric. For. Meteorol.*, 169, 122–135, doi:10.1016/j.agrformet.2012.09.006, 2013.
919
- 920 McKinney, W.: Data Structures for Statistical Computing in Python, in Proceedings of the 9th
921 Python in Science Conference, edited by S. Van Der Walt, pp. 51–56., 2010.
922
- 923 Medlyn, B. E., Duursma, R. A., Eamus, D., Ellsworth, D. S., Prentice, I. C., Barton, C. V. M.,
924 Crous, K. Y., De Angelis, P., Freeman, M. and Wingate, L.: Reconciling the optimal and
925 empirical approaches to modelling stomatal conductance, *Glob. Chang. Biol.*, 17(6), 2134–2144,
926 doi:10.1111/j.1365-2486.2010.02375.x, 2011.
927
- 928 Merbold, L., Eugster, W., Stieger, J., Zahniser, M., Nelson, D. and Buchmann, N.: Greenhouse
929 gas budget (CO₂, CH₄, and N₂O) of intensively managed grassland following restoration, *Glob.*
930 *Chang. Biol.*, 20(6), 1913–1928, doi:10.1111/gcb.12518, 2014.
931
- 932 Migliavacca, M., Meroni, M., Busetto, L., Colombo, R., Zenone, T., Matteucci, G., Manca, G.
933 and Seufert, G.: Modeling gross primary production of agro-forestry ecosystems by assimilation
934 of satellite-derived information in a process-based model, *Sensors*, 9(2), 922–942,
935 doi:10.3390/s90200922, 2009.
936
- 937 Mills, G., Hayes, F., Simpson, D., Emberson, L., Norris, D., Harmens, H. and Büker, P.:
938 Evidence of widespread effects of ozone on crops and (semi-)natural vegetation in Europe
939 (1990–2006) in relation to AOT40- and flux-based risk maps, *Glob. Chang. Biol.*, 17(1), 592–
940 613, doi:10.1111/j.1365-2486.2010.02217.x, 2011.
941
- 942 Monson, R. K., Turnipseed, A. A., Sparks, J. P., Harley, P. C., Scott-Denton, L. E., Sparks, K.
943 and Huxman, T. E.: Carbon sequestration in a high-elevation, subalpine forest, *Glob. Chang.*
944 *Biol.*, 8(5), 459–478, doi:10.1046/j.1365-2486.2002.00480.x, 2002.
945
- 946 Montagnani, L., Manca, G., Canepa, E., Georgieva, E., Acosta, M., Feigenwinter, C., Janous, D.,
947 Kerschbaumer, G., Lindroth, A., Minach, L., Minerbi, S., Mölder, M., Pavelka, M., Seufert, G.,
948 Zeri, M. and Ziegler, W.: A new mass conservation approach to the study of CO₂ advection in
949 an alpine forest, *J. Geophys. Res.*, 114(D7), D07306, doi:10.1029/2008jd010650, 2009.
950
- 951 Monteith, J. L.: Evaporation and surface temperature, *Quarterly J. R. Meteorol. Soc.*, 107(451),
952 1–27, 1981.
953
- 954 Moore, K. E., Fitzjarrald, D. R., Sakai, R. K., Goulden, M. L., Munger, J. W. and Wofsy, S. C.:
955 Seasonal variation in radiative and turbulent exchange at a deciduous forest in central
956 Massachusetts, *J. Appl. Meterology*, 35, 122–134, doi:10.1175/1520-
957 0450(1996)035<0122:SVIRAT>2.0.CO;2, 1996.



- 958
959 Morin, T. H., Bohrer, G., d. M. Frasson, R. P., Naor-Azreli, L., Mesi, S., Stefanik, K. C. and
960 Schäfer, K. V. R.: Environmental drivers of methane fluxes from an urban temperate wetland
961 park, *J. Geophys. Res. Biogeosciences*, 119(11), 2188–2208, doi:10.1002/2014jg002750, 2014.
962 Moureaux, C., Debacq, A., Bodson, B., Heinesch, B. and Aubinet, M.: Annual net ecosystem
963 carbon exchange by a sugar beet crop, *Agric. For. Meteorol.*, 139(1–2), 25–39,
964 doi:10.1016/j.agrformet.2006.05.009, 2006.
965
966 Munger, J. W., Wofsy, S. C., Bakwin, P. S., Fan, S., Goulden, M. L., Daube, B. C., Goldstein, A.
967 H., Moore, K. E. and Fitzjarrald, D. R.: Atmospheric deposition of reactive nitrogen oxides and
968 ozaone in a temperate deciduos forest and a subartic woodland 1. Measurements and
969 mechanisms, *J. Geophys. Res.*, 101, 12639–12657, 1996.
970
971 Musselman, R. C., Lefohn, A. S., Massman, W. J. and Heath, R. L.: A critical review and
972 analysis of the use of exposure- and flux-based ozone indices for predicting vegetation effects,
973 *Atmos. Environ.*, 40(10), 1869–1888, doi:10.1016/j.atmosenv.2005.10.064, 2006.
974
975 Noormets, A., Chen, J. and Crow, T. R.: Age-Dependent Changes in Ecosystem Carbon Fluxes
976 in Managed Forests in Northern Wisconsin, USA, *Ecosystems*, 10(2), 187–203,
977 doi:10.1007/s10021-007-9018-y, 2007.
978
979 Oikawa, P. Y., Jenerette, G. D., Knox, S. H., Sturtevant, C., Verfaillie, J., Dronova, I.,
980 Poindexter, C. M., Eichelmann, E. and Baldocchi, D. D.: Evaluation of a hierarchy of models
981 reveals importance of substrate limitation for predicting carbon dioxide and methane exchange in
982 restored wetlands, *J. Geophys. Res. Biogeosciences*, 122(1), 145–167,
983 doi:10.1002/2016jg003438, 2017.
984
985 Paoletti, E. and Manning, W. J.: Toward a biologically significant and usable standard for ozone
986 that will also protect plants, *Environ. Pollut.*, 150(1), 85–95, doi:10.1016/j.envpol.2007.06.037,
987 2007.
988
989 Papale, D., Migliavacca, M., Cremonese, E., Cescatti, A., Alberti, G., Balzarolo, M., Marchesini,
990 L. B., Canfora, E., Casa, R., Duce, P., Facini, O., Galvagno, M., Genesio, L., Gianelle, D.,
991 Magliulo, V., Matteucci, G., Montagnani, L., Petrella, F., Pitacco, A., Seufert, G., Spano, D.,
992 Stefani, P., Vaccari, F. P. and Valentini, R.: Carbon, water and anergy fluxes of terrestrial
993 ecosystems in Italy, in *The Greenhouse Gas Balance of Italy*, pp. 11–45, Springer, Berlin
994 Heidelberg., 2015.
995
996 Pastorello, G., Agarwal, D., Papale, D., Samak, T., Trotta, C., Ribeca, A., Poindexter, C.,
997 Faybishenko, B., Gunter, D., Hollowgrass, R. and Canfora, E.: Observational data patterns for
998 time series data quality assessment, 2014 IEEE 10th Int. Conf. e-Science, 271–278,
999 doi:10.1109/eScience.2014.45, 2014.
1000
1001 Pastorello, G., Papale, D., Chu, H., Trotta, C., Agarwal, D., Canfora, E., Baldocchi, D. and Torn,
1002 M.: A new data set to keep a sharper eye on land-air exchanges, *Eos (Washington. DC.)*, 98,
1003 doi:10.1029/2017EO071597, 2017.



- 1004
1005 Pleijel, H., Danielsson, H., Ojanperä, K., De Temmerman, L., Högy, P., Badiani, M. and
1006 Karlsson, P. E.: Relationships between ozone exposure and yield loss in European wheat and
1007 potato - A comparison of concentration- and flux-based exposure indices, *Atmos. Environ.*,
1008 38(15), 2259–2269, doi:10.1016/j.atmosenv.2003.09.076, 2004.
1009
1010 Pleijel, H., Danielsson, H., Simpson, D. and Mills, G.: Have ozone effects on carbon
1011 sequestration been overestimated? A new biomass response function for wheat, *Biogeosciences*,
1012 11(16), 4521–4528, doi:10.5194/bg-11-4521-2014, 2014.
1013
1014 Pilegaard, K., Ibrøm, A., Courtney, M. S., Hummelshøj, P. and Jensen, N. O.: Increasing net
1015 CO₂ uptake by a Danish beech forest during the period from 1996 to 2009, *Agric. For.*
1016 *Meteorol.*, 151(7), 934–946, doi:10.1016/j.agrformet.2011.02.013, 2011.
1017
1018 Post, H., Franssen, H. J. H., Graf, A., Schmidt, M. and Vereecken, H.: Uncertainty analysis of
1019 eddy covariance CO₂ flux measurements for different EC tower distances using an extended
1020 two-tower approach, *Biogeosciences*, 12(4), 1205–1221, doi:10.5194/bg-12-1205-2015, 2015.
1021
1022 Powell, T. L., Bracho, R., Li, J., Dore, S., Hinkle, C. R. and Drake, B. G.: Environmental
1023 controls over net ecosystem carbon exchange of scrub oak in central Florida, *Agric. For.*
1024 *Meteorol.*, 141(1), 19–34, doi:10.1016/j.agrformet.2006.09.002, 2006.
1025
1026 Prescher, A.-K., Grünwald, T. and Bernhofer, C.: Land use regulates carbon budgets in eastern
1027 Germany: From NEE to NBP, *Agric. For. Meteorol.*, 150(7–8), 1016–1025,
1028 doi:10.1016/j.agrformet.2010.03.008, 2010.
1029
1030 Rambal, S., Joffre, R., Ourcival, J. M., Cavender-Bares, J. and Rocheteau, A.: The growth
1031 respiration component in eddy CO₂ flux from a *Quercus ilex* mediterranean forest, *Glob. Chang.*
1032 *Biol.*, 10(9), 1460–1469, doi:10.1111/j.1365-2486.2004.00819.x, 2004.
1033
1034 Rannik, Ü., Mammarella, I., Keronen, P. and Vesala, T.: Vertical advection and nocturnal
1035 deposition of ozone over a boreal pine forest, *Atmos. Chem. Phys.*, 9(6), 2089–2095,
1036 doi:10.5194/acp-9-2089-2009, 2009.
1037
1038 Rannik, Ü., Altimir, N., Mammarella, I., Bäck, J., Rinne, J., Ruuskanen, T. M., Hari, P., Vesala, T.
1039 and Kulmala, M.: Ozone deposition into a boreal forest over a decade of observations:
1040 Evaluating deposition partitioning and driving variables, *Atmos. Chem. Phys.*, 12(24), 12165–
1041 12182, doi:10.5194/acp-12-12165-2012, 2012.
1042
1043 Raz-Yaseef, N., Billesbach, D. P., Fischer, M. L., Biraud, S. C., Gunter, S. A., Bradford, J. A.
1044 and Torn, M. S.: Vulnerability of crops and native grasses to summer drying in the U.S. Southern
1045 Great Plains, *Agric. Ecosyst. Environ.*, 213, 209–218, doi:10.1016/j.agee.2015.07.021, 2015.
1046
1047 Reda, I. and Andreas, A.: Solar position algorithm for solar radiation applications, *Sol. Energy*,
1048 76(5), 577–589, doi:10.1016/j.solener.2003.12.003, 2004.
1049



- 1050 Reich, P. B.: Quantifying plant response to ozone: A unifying theory, *Tree Physiol.*, 3(0), 63–91,
1051 doi:10.1093/treephys/3.1.63, 1987.
1052
1053 Reich, P. B. and Amundson, R. G.: Ambient levels of ozone reduce net photosynthesis in tree
1054 and crop species, *Science* (80-.), 230(11), 566–570, 1985.
1055
1056 Reich, P. B. and Lassoie, J. P.: Effects of low level O₃ exposure on leaf diffusive conductance
1057 and water-use efficiency in hybrid poplar, *Plant. Cell Environ.*, 7(9), 661–668,
1058 doi:10.1111/1365-3040.ep11571645, 1984.
1059
1060 Reichstein, M., Falge, E., Baldocchi, D., Papale, D., Aubinet, M., Berbigier, P., Bernhofer, C.,
1061 Buchmann, N., Gilmanov, T., Granier, A., Grünwald, T., Havráneková, K., Ilvesniemi, H.,
1062 Janous, D., Knöhl, A., Laurila, T., Lohila, A., Loustau, D., Matteucci, G., Meyers, T., Miglietta,
1063 F., Ourcival, J. M., Pumpanen, J., Rambal, S., Rotenberg, E., Sanz, M., Tenhunen, J., Seufert, G.,
1064 Vaccari, F., Vesala, T., Yakir, D. and Valentini, R.: On the separation of net ecosystem exchange
1065 into assimilation and ecosystem respiration: Review and improved algorithm, *Glob. Chang. Biol.*,
1066 11(9), 1424–1439, doi:10.1111/j.1365-2486.2005.001002.x, 2005.
1067
1068 Reverter, B. R., Sánchez-Cañete, E. P., Resco, V., Serrano-Ortiz, P., Oyonarte, C. and Kowalski,
1069 A. S.: Analyzing the major drivers of NEE in a Mediterranean alpine shrubland, *Biogeosciences*,
1070 7(9), 2601–2611, doi:10.5194/bg-7-2601-2010, 2010.
1071
1072 Rey, A., Pegoraro, E., Tedeschi, V., Parri, I. De, Jarvis, P. G. and Valentini, R.: Annual variation
1073 in soil respiration and its components in a coppice oak forest in Central Italy, *Glob. Chang. Biol.*,
1074 8(9), 851–866, doi:10.1046/j.1365-2486.2002.00521.x, 2002.
1075
1076 Ruehr, N. K., Martin, J. G. and Law, B. E.: Effects of water availability on carbon and water
1077 exchange in a young ponderosa pine forest: Above- and belowground responses, *Agric. For. Meteorol.*,
1078 164, 136–148, doi:10.1016/j.agrformet.2012.05.015, 2012.
1079
1080 Sabbatini, S., Arriga, N., Bertolini, T., Castaldi, S., Chiti, T., Consalvo, C., Djomo, S. N., Gioli,
1081 B., Matteucci, G. and Papale, D.: Greenhouse gas balance of cropland conversion to bioenergy
1082 poplar short-rotation coppice, *Biogeosciences*, 13(1), 95–113, doi:10.5194/bg-13-95-2016, 2016.
1083
1084 Schmidt, M., Reichenau, T. G., Fiener, P. and Schneider, K.: The carbon budget of a winter
1085 wheat field: An eddy covariance analysis of seasonal and inter-annual variability, *Agric. For. Meteorol.*,
1086 165, 114–126, doi:10.1016/j.agrformet.2012.05.012, 2012.
1087
1088 Schnell, J. L., Holmes, C. D., Jangam, A. and Prather, M. J.: Skill in forecasting extreme ozone
1089 pollution episodes with a global atmospheric chemistry model, *Atmos. Chem. Phys.*, 14(15),
1090 7721–7739, doi:10.5194/acp-14-7721-2014, 2014.
1091
1092 Schwede, D., Zhang, L., Vet, R. and Lear, G.: An intercomparison of the deposition models used
1093 in the CASTNET and CAPMoN networks, *Atmos. Environ.*, 45(6), 1337–1346,
1094 doi:10.1016/j.atmosenv.2010.11.050, 2011.
1095



- 1096 Scott, R. L., Jenerette, G. D., Potts, D. L. and Huxman, T. E.: Effects of seasonal drought on net
1097 carbon dioxide exchange from a woody-plant-encroached semiarid grassland, *J. Geophys. Res.*,
1098 114(G4), G04004, doi:10.1029/2008jg000900, 2009.
1099
- 1100 Scott, R. L., Hamerlynck, E. P., Jenerette, G. D., Moran, M. S. and Barron-Gafford, G. A.:
1101 Carbon dioxide exchange in a semidesert grassland through drought-induced vegetation change,
1102 *J. Geophys. Res.*, 115(G3), G03026, doi:10.1029/2010jg001348, 2010.
1103
- 1104 Scott, R. L., Biederman, J. A., Hamerlynck, E. P. and Barron-Gafford, G. A.: The carbon balance
1105 pivot point of southwestern U.S. semiarid ecosystems: Insights from the 21st century drought, *J.*
1106 *Geophys. Res. Biogeosciences*, 120(12), 2612–2624, doi:10.1002/2015jg003181, 2015.
1107
- 1108 Seabold, S. and Perktold, J.: Statsmodels: econometric and statistical modeling with Python, in
1109 Proceedings of the 9th Python in Science Conference, pp. 57–61. [online] Available from:
1110 <http://conference.scipy.org/proceedings/scipy2010/pdfs/seabold.pdf> %Cn<http://conference.scipy.org/proceedings/scipy2010/seabold.html>, 2010.
1111
- 1112
- 1113 Sen, P. K.: Estimates of the regression coefficient based on Kendall's tau, *J. Am. Stat. Assoc.*,
1114 63(324), 1379–1389, doi:10.1080/01621459.1968.10480934, 1968.
1115
- 1116 Silva, S. J. and Heald, C. L.: Investigating dry deposition of ozone to vegetation, *J. Geophys.*
1117 *Res. Atmos.*, 123, 559–573, doi:10.1002/2017JD027278, 2018.
1118
- 1119 Sitch, S., Cox, P. M., Collins, W. J. and Huntingford, C.: Indirect radiative forcing of climate
1120 change through ozone effects on the land-carbon sink., *Nature*, 448, 791–794,
1121 doi:10.1038/nature06059, 2007.
1122
- 1123 Stella, P., Personne, E., Loubet, B., Lamaud, E., Ceschia, E., Béziat, P., Bonnefond, J. M., Irvine,
1124 M., Keravec, P., Mascher, N. and Cellier, P.: Predicting and partitioning ozone fluxes to maize
1125 crops from sowing to harvest: The Surfamt-O 3 model, *Biogeosciences*, 8(10), 2869–2886,
1126 doi:10.5194/bg-8-2869-2011, 2011.
1127
- 1128 Stella, P., Kortner, M., Ammann, C., Foken, T., Meixner, F. X. and Trebs, I.: Measurements of
1129 nitrogen oxides and ozone fluxes by eddy covariance at a meadow: Evidence for an internal leaf
1130 resistance to NO₂, *Biogeosciences*, 10(9), 5997–6017, doi:10.5194/bg-10-5997-2013, 2013.
1131
- 1132 Sulman, B. N., Desai, A. R., Cook, B. D., Saliendra, N. and Mackay, D. S.: Contrasting carbon
1133 dioxide fluxes between a drying shrub wetland in Northern Wisconsin, USA, and nearby forests,
1134 *Biogeosciences*, 6(6), 1115–1126, doi:10.5194/bg-6-1115-2009, 2009.
1135
- 1136 Tai, A. P. K., Martin, M. V. and Heald, C. L.: Threat to future global food security from climate
1137 change and ozone air pollution, *Nat. Clim. Chang.*, 4, 817–821, doi:10.1038/nclimate2317, 2014.
1138
- 1139 Taylor, J. R.: An Introduction to Error Analysis, University Science Books, Sausalito., 1997.
1140
- 1141 Tedeschi, V., Ret, A., Manca, G., Valentini, R., Jarvis, P. G. and Borghetti, M.: Soil respiration



- 1142 in a Mediterranean oak forest at different developmental stages after coppicing, *Glob. Chang. Biol.*, 12(1), 110–121, doi:10.1111/j.1365-2486.2005.01081.x, 2006.
- 1143
- 1144
- 1145 Thum, T., Aalto, T., Laurila, T., Aurela, M., Kolari, P. and Hari, P.: Parametrization of two
1146 photosynthesis models at the canopy scale in a northern boreal Scots pine forest, *Tellus B*, 59(5),
1147 doi:10.3402/tellusb.v59i5.17066, 2007.
- 1148
- 1149 UNECE: Revised manual on methodologies and criteria for mapping critical levels/loads and
1150 geographical areas where they are exceeded, in UNECE Convention on Long-range
1151 Transboundary Air Pollution., 2004.
- 1152
- 1153 Urbanski, S., Barford, C., Wofsy, S., Kucharik, C., Pyle, E., Budney, J., McKain, K., Fitzjarrald,
1154 D., Czikowsky, M. and Munger, J. W.: Factors controlling CO₂ exchange on timescales from
1155 hourly to decadal at Harvard Forest, *J. Geophys. Res.*, 112(G2), G02020,
1156 doi:10.1029/2006jg000293, 2007.
- 1157
- 1158 Valentini, R., Angelis, P., Matteucci, G., Monaco, R., Dore, S. and Mucnozza, G. E. S.: Seasonal
1159 net carbon dioxide exchange of a beech forest with the atmosphere, *Glob. Chang. Biol.*, 2(3),
1160 199–207, doi:10.1111/j.1365-2486.1996.tb00072.x, 1996.
- 1161
- 1162 Verma, S. B., Dobermann, A., Cassman, K. G., Walters, D. T., Knops, J. M., Arkebauer, T. J.,
1163 Suyker, A. E., Burba, G. G., Amos, B., Yang, H., Ginting, D., Hubbard, K. G., Gitelson, A. A.
1164 and Walter-Shea, E. A.: Annual carbon dioxide exchange in irrigated and rainfed maize-based
1165 agroecosystems, *Agric. For. Meteorol.*, 131(1–2), 77–96, doi:10.1016/j.agrformet.2005.05.003,
1166 2005.
- 1167
- 1168 Vitale, L., Tommasi, P. Di, D'Urso, G. and Magliulo, V.: The response of ecosystem carbon
1169 fluxes to LAI and environmental drivers in a maize crop grown in two contrasting seasons, *Int. J.*
1170 *Biometeorol.*, 60(3), 411–420, doi:10.1007/s00484-015-1038-2, 2015.
- 1171
- 1172 Vuichard, N. and Papale, D.: Filling the gaps in meteorological continuous data measured at
1173 FLUXNET sites with ERA-Interim reanalysis, *Earth Syst. Sci. Data*, 7(2), 157–171,
1174 doi:10.5194/essd-7-157-2015, 2015.
- 1175
- 1176 Van Der Walt, S., Colbert, S. C. and Varoquaux, G.: The NumPy array: A structure for efficient
1177 numerical computation, *Comput. Sci. Eng.*, 13(2), 22–30, doi:10.1109/MCSE.2011.37, 2011.
- 1178
- 1179 Warton, D. I., IJ, W., DS, F. and M, W.: Bivariate line-fitting methods for allometry, *Biol Rev*,
1180 81, 259–291, doi:10.1017/S1464793106007007, 2006.
- 1181
- 1182 Weaver, J. E. and Bruner, W. E.: Root development of vegetable crops, McGraw-Hill Book
1183 Company, Inc., Lincoln, Nebraska., 1927.
- 1184
- 1185 Wesely, M. L. and Hicks, B. B.: Some factors that affect the deposition rates of sulfur dioxide
1186 and similar gases on vegetation, *J. Air Pollut. Control Assoc.*, 27(11), 1110–1116,
1187 doi:10.1080/00022470.1977.10470534, 1977.



- 1188
1189 Wesley, M. L.: Parametrization of surface resistance to gaseous dry deposition in regional-scale
1190 numerical model, *Atmos. Environ.*, 23(6), 1293–1304, 1989.
1191
1192 Wittig, V. E., Ainsworth, E. A. and Long, S. P.: To what extent do current and projected
1193 increases in surface ozone affect photosynthesis and stomatal conductance of trees? A meta-
1194 analytic review of the last 3 decades of experiments, *Plant, Cell Environ.*, 30(9), 1150–1162,
1195 doi:10.1111/j.1365-3040.2007.01717.x, 2007.
1196
1197 Wittig, V. E., Ainsworth, E. A., Naidu, S. L., Karnosky, D. F. and Long, S. P.: Quantifying the
1198 impact of current and future tropospheric ozone on tree biomass, growth, physiology and
1199 biochemistry: A quantitative meta-analysis, *Glob. Chang. Biol.*, 15(2), 396–424,
1200 doi:10.1111/j.1365-2486.2008.01774.x, 2009.
1201
1202 Wohlfahrt, G., Hammerle, A., Haslwanter, A., Bahn, M., Tappeiner, U. and Cernusca, A.:
1203 Seasonal and inter-annual variability of the net ecosystem CO₂ exchange of a temperate
1204 mountain grassland: Effects of weather and management, *J. Geophys. Res.*, 113(D8), D08110,
1205 doi:10.1029/2007jd009286, 2008.
1206
1207 Wu, S., Mickley, L. J., Jacob, D. J., Logan, J. A., Yantosca, R. M. and Rind, D.: Why are there
1208 large differences between models in global budgets of tropospheric ozone?, *J. Geophys. Res.*
1209 *Atmos.*, 112, D05302, doi:10.1029/2006JD007801, 2007.
1210
1211 Young, P. J., Archibald, A. T., Bowman, K. W., Lamarque, J.-F., Naik, V., Stevenson, D. S.,
1212 Tilmes, S., Voulgarakis, A., Wild, O., Bergmann, D., Cameron-Smith, P., Cionni, I., Collins, W.
1213 J., Dalsøren, S. B., Doherty, R. M., Eyring, V., Faluvegi, G., Horowitz, L. W., Josse, B., Lee, Y.
1214 H., MacKenzie, I. A., Nagashima, T., Plummer, D. A., Righi, M., Rumbold, S. T., Skeie, R. B.,
1215 Shindell, D. T., Strode, S. A., Sudo, K., Szopa, S. and Zeng, G.: Pre-industrial to end 21st
1216 century projections of tropospheric ozone from the Atmospheric Chemistry and Climate Model
1217 Intercomparison Project (ACCMIP), *Atmos. Chem. Phys.*, 13(4), 2063–2090, doi:10.5194/acp-
1218 13-2063-2013, 2013.
1219
1220 Yue, X. and Unger, N.: Ozone vegetation damage effects on gross primary productivity in the
1221 United States, *Atmos. Chem. Phys.*, 14(17), 9137–9153, doi:10.5194/acp-14-9137-2014, 2014.
1222
1223 Yue, X., Keenan, T. F., Munger, W. and Unger, N.: Limited effect of ozone reductions on the
1224 20-year photosynthesis trend at Harvard forest, *Glob. Chang. Biol.*, 22(11), 3750–3759,
1225 doi:10.1111/gcb.13300, 2016.
1226
1227 Zeller, K. F. and Nikolov, N. T.: Quantifying simultaneous fluxes of ozone , carbon dioxide and
1228 water vapor above a subalpine forest ecosystem, *Environ. Pollut.*, 107, 1–20, 2000.
1229
1230 Zhang, L., Brook, J. R. and Vet, R.: On ozone dry deposition - With emphasis on non-stomatal
1231 uptake and wet canopies, *Atmos. Environ.*, 36(30), 4787–4799, doi:10.1016/S1352-
1232 2310(02)00567-8, 2002.
1233



- 1234 Zhang, L., Brook, J. R. and Vet, R.: A revised parameterization for gaseous dry deposition in air-
1235 quality models, *Atmos. Chem. Phys. Discuss.*, 3(2), 1777–1804, doi:10.5194/acpd-3-1777-2003,
1236 2003.
1237
1238 Zielis, S., Etzold, S., Zweifel, R., Eugster, W., Haeni, M. and Buchmann, N.: NEP of a Swiss
1239 subalpine forest is significantly driven not only by current but also by previous years weather,
1240 *Biogeosciences*, 11(6), 1627–1635, doi:10.5194/bg-11-1627-2014, 2014.
1241
1242 Zona, D., Gioli, B., Fares, S., De Groote, T., Pilegaard, K., Ibrom, A. and Ceulemans, R.:
1243 Environmental controls on ozone fluxes in a poplar plantation in Western Europe, *Environ.*
1244 *Pollut.*, 184, 201–210, doi:10.1016/j.envpol.2013.08.032, 2014.
1245
1246



1247 Table 1. Description of sites that measure O₃ flux and their daytime growing season (April-
 1248 September) conditions ^a
 1249

	Blodgett Forest, California, USA	Hyytiälä Forest, Finland	Harvard Forest, Massachusetts, USA
Latitude, Longitude	38.8953, -120.6328	61.8475, 24.2950	42.5378, -72.1715
Plant functional type	Evergreen needleleaf	Evergreen needleleaf	Deciduous broadleaf
Years of data	2001-2007	2007-2012	1993-1999
Days of observations	1281	1098	1281
Canopy height, m	8	15	24
GPP, $\mu\text{mol m}^{-2} \text{s}^{-1}$	9.22 ± 3.55	11.1 ± 5.02	12.4 ± 7.62
ET, $\text{mmol m}^{-2} \text{s}^{-1}$	3.25 ± 1.23	1.71 ± 0.82	2.95 ± 1.70
PAR, $\mu\text{mol m}^{-2} \text{s}^{-1}$	875 ± 149	690 ± 203	876 ± 222
Air Temperature, °C	19.1 ± 5.36	13.3 ± 5.99	17.65 ± 5.75
VPD, kPa	1.51 ± 0.61	0.73 ± 0.32	0.90 ± 0.34
O ₃ , ppb	55.4 ± 13.4	32.2 ± 8.68	48.8 ± 15.8
F_{s,O_3} , nmol m ⁻² s ⁻¹	5.18 ± 2.11	4.35 ± 1.66	7.23 ± 4.87
Precipitation, mm day ⁻¹	0.09 ± 0.49	0.42 ± 0.89	0.28 ± 0.82

1250
 1251 ^a Values are mean ± standard deviation of daily averages, using daytime observations only. GPP is gross
 1252 primary productivity. ET is evapotranspiration. PAR is photosynthetically active radiation. VPD is vapor
 1253 pressure deficit. F_{s,O_3} is observed stomatal O₃ flux.
 1254
 1255
 1256
 1257
 1258
 1259

1260 Table 2. Mean O₃ SynFlux, deposition velocity and its conductance components during daytime
 1261 in the growing season (April-September), grouped by plant functional type (PFT).^a
 1262

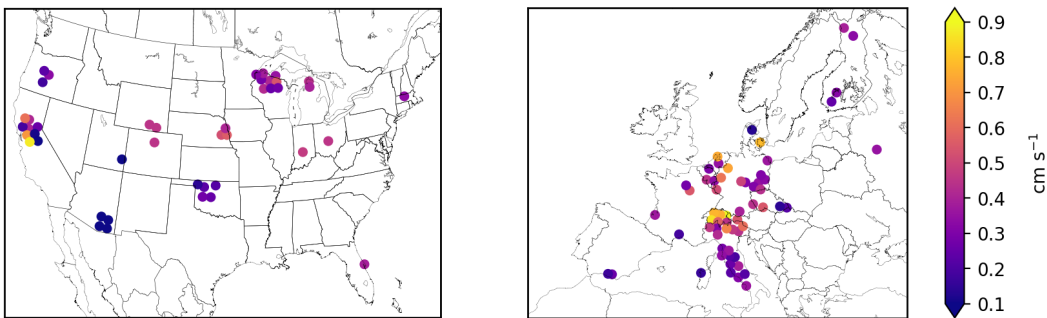
PFT ^b	Sites	Site-Years	g_s	g_{ns}	g_c	v_d	F'_{O_3}	F'_{s,O_3}	CUO	CUO3
CRO	18	148	0.42±0.17	0.28±0.09	0.68±0.18	0.53±0.12	7.66±1.96	4.77±1.52	24.8±12.4	14.9±9.3
ENF	25	254	0.37±0.10	0.25±0.06	0.60±0.11	0.54±0.10	7.37±1.33	4.61±1.16	20.0±5.69	11.9±6.30
EBF	3	31	0.21±0.02	0.15±0.02	0.36±0.03	0.33±0.03	5.02±0.65	2.90±0.28	12.1±0.81	5.12±0.45
DBF	16	158	0.41±0.14	0.20±0.09	0.60±0.18	0.53±0.15	7.87±2.28	5.37±1.69	28.6±13.8	15.7±6.66
MF	5	83	0.44±0.17	0.19±0.01	0.62±0.15	0.56±0.14	7.82±1.91	5.53±2.15	24.9±10.5	15.9±8.90
WSA	2	25	0.10±0.02	0.31±0.06	0.39±0.04	0.36±0.04	6.14±0.20	1.47±0.31	6.46±1.43	2.54±1.72
OSH	4	14	0.19±0.07	0.29±0.10	0.47±0.10	0.41±0.09	5.69±1.33	2.23±0.87	8.60±3.27	2.27±1.54
CSH	2	15	0.27±0.11	0.29±0.01	0.57±0.09	0.49±0.05	6.78±0.95	3.34±1.24	14.3±5.30	7.62±5.49
GRA	18	136	0.40±0.30	0.24±0.11	0.64±0.26	0.47±0.15	7.04±7.04	4.12±2.45	18.3±10.7	9.90±6.98
WET	10	53	0.48±0.16	0.27±0.09	0.74±0.21	0.58±0.14	8.80±2.74	5.77±2.08	25.1±9.65	19.4±15.6

1263
 1264 ^a Values are the mean ± standard deviation across sites within each PFT. Units for g_s , g_{ns} , g_c , and v_d are cm
 1265 s^{-1} . Units for F'_{O_3} and F'_{s,O_3} are nmol m⁻² s⁻¹.

1266 ^b CRO = crop, ENF = evergreen needleleaf forest, EBF = evergreen broadleaf forest, DBF = deciduous
 1267 broadleaf forest, MF = mixed forest, WSA = woody savanna, OSH = open shrubland, CSH = closed
 1268 shrubland, GRA = grassland, WET = wetland



1269



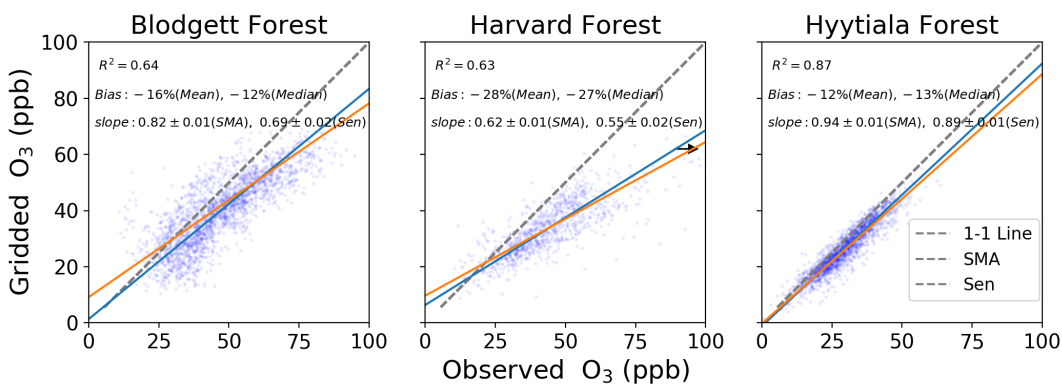
1270

1271

1272 Figure 1. Mean stomatal conductance for O₃ (g_s) during daytime in the growing season (April-
1273 September) at FLUXNET2015 sites in the United States and Europe. Symbols of some sites have
1274 been moved slightly to reduce overlap and improve legibility.

1275

1276



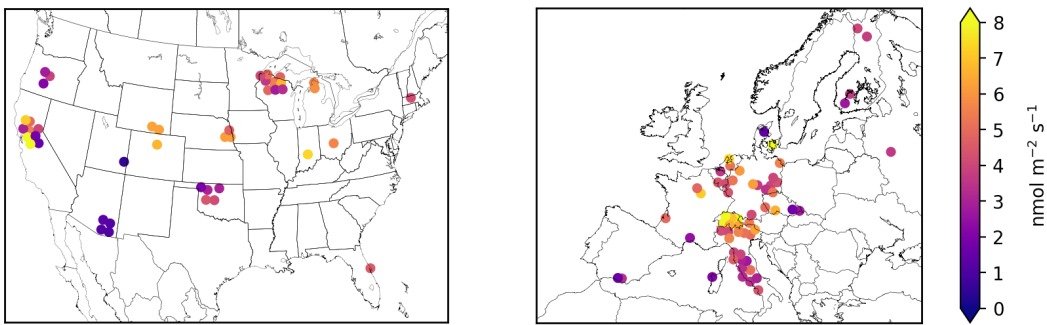
1277

1278

1279 Figure 2. Gridded and observed daily daytime O₃ concentrations at Blodgett, Harvard, and
1280 Hyytiälä Forests. Inset numbers provide the coefficient of determination (R²), mean and median
1281 bias, the standard major axis (SMA) slope, the Thiel-Sen (Sen) slope, and the 68% confidence
1282 interval of the slopes. Black arrow points towards outliers that are not shown.
1283

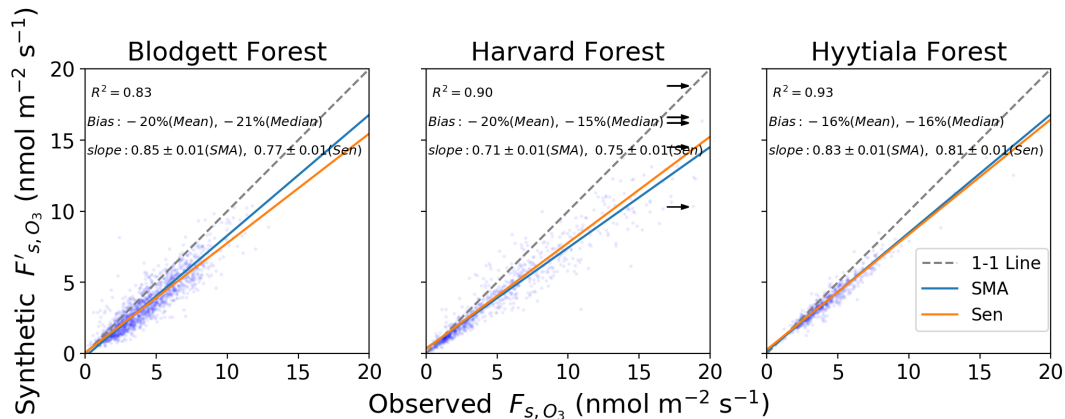


1284



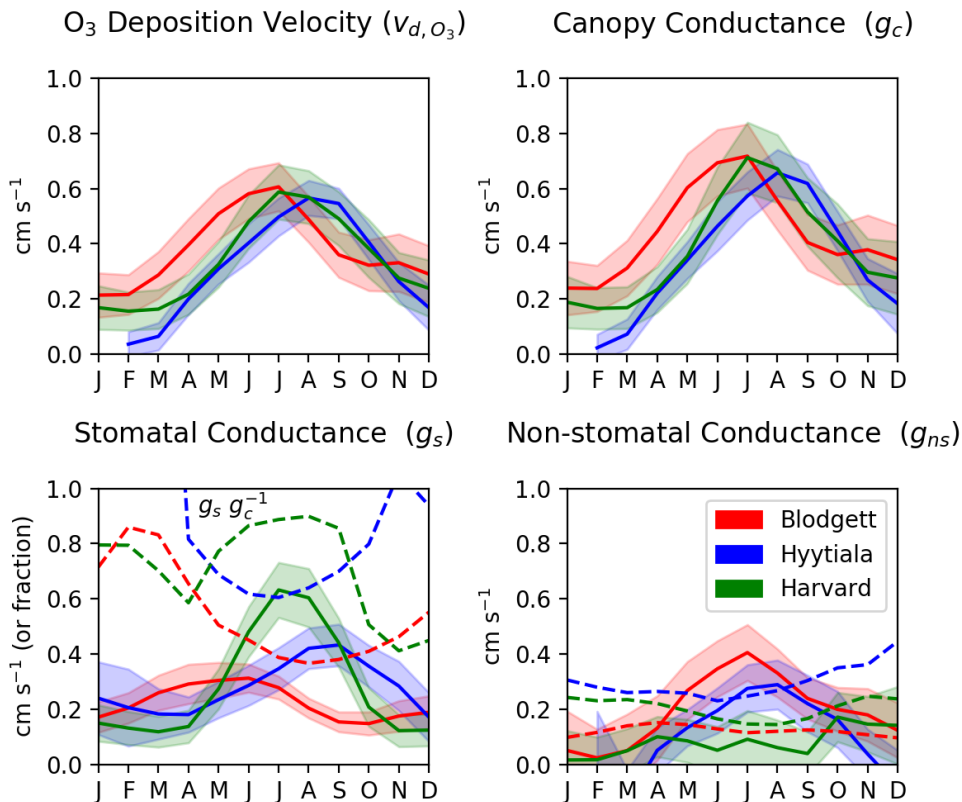
1285
 1286
 1287
 1288
 1289
 1290

Figure 3. Mean synthetic stomatal O₃ flux (F'_{s,O_3} , Sect. 2.1) during the daytime growing season (April-September) at FLUXNET2015 sites in the United States and Europe. Symbols of some sites have been moved slightly to reduce overlap and improve legibility.

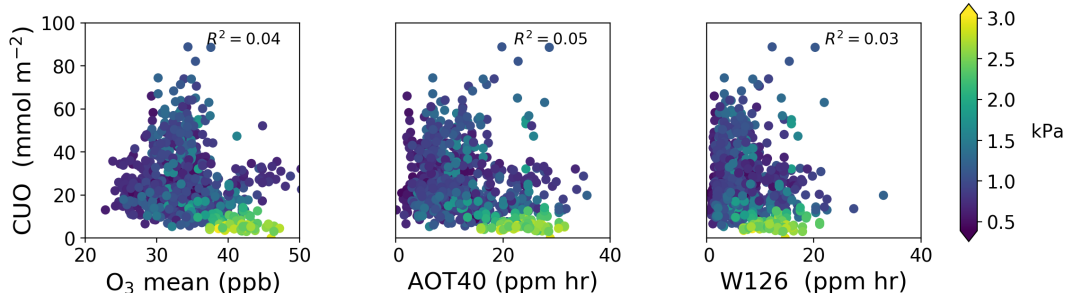


1291
 1292
 1293

Figure 4. Synthetic and observed daily daytime stomatal O₃ flux. See Sect. 2.1 for definition of F'_{s,O_3} and Fig. 2 for explanation of lines and inset text.



1294
 1295 Figure 5. Observed O₃ deposition velocity and its in-canopy components at sites with O₃ flux
 1296 measurements. Lines show means and shaded regions show standard deviation of daily values
 1297 for each month. Dashed lines on the stomatal conductance panel show the stomatal fraction of
 1298 total canopy conductance ($g_s g_c^{-1}$) and dashed lines on the non-stomatal conductance panel show
 1299 the parameterized value.



1300
1301
1302
1303
1304
1305
1306

Figure 6. Comparison of cumulative uptake of O_3 (CUO) to concentration-based metrics of O_3 exposure during the daytime growing season (April-September) at 103 sites: mean O_3 concentration (left), AOT40 (center), and W126 (right). There is one value (dot) per site per year. Colors show mean vapor pressure deficit during the growing season.